Development and characterization of nanovesicles and colloidosomes for small-molecule delivery

by

Bennett Uhl

B.S., Kansas State University, 2017

A THESIS

submitted in partial fulfillment of the requirements for the degree

MASTER OF SCIENCE

Department of Animal Sciences
College of Agriculture

KANSAS STATE UNIVERSITY
Manhattan, Kansas

2019

Approved by:

Major Professor
Dr. Umut Yucel

Abstract

Controlled diffusion of bioactive ingredients is of interest to food, cosmetic, and drug industries. To characterize delivery systems and interactions with small molecules, a model hydrophobic molecule, 4-phenyl-2,2,5,5-tetramethyl-3-imidazoline-1-oxyl nitroxide (PTMIO), which is an electron paramagnetic resonance (EPR)-active spin probe was used. The objectives of this research were to study (1) the effect of a solid fat barrier to NLC on the diffusion of PTMIO and (2) how the fatty acid packaging of phospholipid structures affects the release of PTMIO from liposomal vesicles (LV).

Colloidosomes, microcapsules with a self-assembled coating, were formed to study the effect of a solid barrier on diffusion. Liquid lipid nanoparticles (LLN; refined coconut oil stabilized by lecithin) and solid lipid nanoparticles (SLN; palm oil stabilized by caseinate) were prepared by high pressure homogenization. Dispersions were adjusted above and below the isoelectric point of caseinate (pH 3.5 and 7) to form colloidosomes. Self-assembly of SLN onto the surface of LLN was studied by controlled mixing of the ratios (2:1 to 1:5) (LLN:SLN) of the two dispersions. Particle size and zeta potential were found by dynamic light scattering (DLS) and phase-analysis light scattering (PALS), respectively. The average zeta potential of LLN was -43.61 ± 2.28 mV at both pHs while SLN was 46.71 ± 5.93 mV at pH 3.5 and -42.74 ± 5.58 mV at pH 7. At a volumetric ratio of (1:3) (LLN:SLN), the mixture appeared to have self-assembled, without evidence of bridging flocculation. The mixture was 431.03 ± 7.2 nm in diameter and had a zeta potential of 32.48 ± 2.01 mV at pH 3.5, with a particle size significantly larger than either LLN or SLN ($p < 0.05$) at pH 3.5, suggesting the particles aggregated. LLN and the mixture were characterized for diffusion by adding PTMIO. PTMIO was reduced by ascorbate and monitored with EPR *in-situ.* PTMIO was quenched significantly slower in colloidosomes at pH

3.5 than at pH 7 ($p < 0.05$). EPR spectra were simulated by a downhill simplex to separate fractions of PTMIO at the lipid and aqueous phases. Diffusion of PTMIO was limited from colloidosomes at pH 3.5.

Saturated (80H or 90H) and unsaturated (PC75 or 90G) phospholipids were used to make nanovesicles to study LV. Because LV can change morphology as molecules are incorporated, a carrier lipid (refined coconut oil), was added at 0, 0.5, or 1.0% to LV before homogenization. LV particle size and zeta potential were characterized by DLS and PALS, respectively. All phospholipids increased in particle size with carrier lipid fraction ($p < 0.05$). Zeta potential differed by phospholipid ($p < 0.05$); however, all LV with negative voltages. Differential scanning calorimetry was used to characterize LV. Crystallization of 90H lecithin onset at ca. 53°C and extended from ca. 45°C to 43°C with the addition of carrier lipid. To study diffusion, PTMIO was loaded into LV and studied by the aforementioned EPR method. Carrier lipid fraction did not affect the diffusion ($p > 0.05$). Reduction of PTMIO in 90H LV was slower than other phospholipids ($p > 0.05$).

Table of Contents

List of Figures

List of Tables

Acknowledgements

I would like to my major advisor Dr. Umut Yucel for his guidance and patience during my graduate studies. I would like to thank Drs. Jayendra Amamcharla, Fadi Aramouni, and Stefan Bossmann for serving on my committee. I am grateful for my family, and the many people who have guided me and provided support at the Food Science Institute at Kansas State University.

1. Review of the Literature

1.1. Overview of delivery systems

Many small molecules can be added to foods to add functionality, which in turn, can add desirable characteristics to products such as flavors, colors, or antioxidants. These small molecules are largely hydrophobic and associate in hydrophobic environments, although lesser solubility in hydrophilic environments occurs depending on the partitioning behavior (e.g., log *P* value). The log *P* value is the tendency to associate in hydrophobic or hydrophilic environments and can be considered in the partitioning coefficient, which is classically the ratio of concentrations of a molecule's solubility both in octanol and in water. Because many small molecules are largely hydrophobic, a delivery system is needed to incorporate them into other products. In addition, many flavor molecules used in foods have reactive functional groups such as aldehydes (e.g., cinnamaldehyde) or ketones (e.g., menthone).

Small molecules may be labile during processing, such as exposure to high heat, without the addition of a delivery system. One instability in the oxidation from the formation of hydrogen peroxide in foods [1]. Oxidation of bioactive components can make foods unacceptable to consumers. Drugs may also be chemically labile without the addition of a delivery system [2].

Hydrophobic and hydrophilic molecules will not readily mix, a substance is needed to reduce the interfacial tension between the two, otherwise immiscible, systems together. The IUPAC calls these molecules surfactants, which are substances that lower the surface tension of the solvent and interfacial tension of the solvent and other phases [3]. According to McClements et al. common surfactant components of delivery system in food systems are lipids (e.g., fish or plant oils), small molecules (e.g., ionic or nonionic compounds), and biopolymers (e.g., proteins

or polysaccharides) [4]. Dispersing the two phases creates many small particles, which increases the surface area of the dispersed phase within the continuous phase.

The increase in surface area is expected to increase the bioavailability of the encapsulated ingredients [5]. To understand the likely fate of encapsulated bioactive molecules, simulated digestion can be used to understand the delivery of these ingredients in the human gastrointestinal tract. Simulated digestion of β-carotene-containing small (0.2 μm diameter), medium (0.4 μm diameter), and large (23 μm diameter) particles showed that smaller particles were more available for lipid digestion and more efficient at releasing encapsulated β-carotene [6]. Further decreasing particle size to the nanoscale (i.e., below 200 nm in diameter) of resveratrol-containing emulsions also increased the bioavailability of resveratrol encapsulated into nanoemulsions [7].

This section discusses delivery systems for small molecules which have been previously studied, their properties and characterization. It then shifts to characterization techniques that are used to evaluate the ability of these systems to carry molecules. Lastly, the use of electron paramagnetic resonance (EPR) spectroscopy to characterize a model hydrophobic ingredient *in-situ* is discussed.

1.2. Emulsion-based delivery systems

Emulsions are a common delivery system used in food applications. Emulsions are named by describing what is dispersed into what, e.g., an oil in water emulsion describes a dispersion where an oil is dispersed into an aqueous continuous phase. For oil in water emulsions, because the surfactant has solubility in both water and oil, it is able to reduce the tension between the two phases by allowing the water-soluble portion to associate at the polar

head and the lipid-soluble region to associate in the lipid tail. One such class of molecules is in surfactants is phospholipids, which are a glycerol with fatty acids occupying two positions and a phosphate attached to the third opening [8]. Another type of emulsion is emulsions that are stabilized by colloidal particles, which is the case for Pickering emulsions [9]. Solid particles in Pickering emulsions reduce the surface tension between the two phases.

To create emulsion particles, it is necessary to use a means of reducing the particle size. Chemical methods can be effective, a major drawback is that they often require the use of an organic solvent, which can remain in the final dispersion [10]. Chemical homogenization techniques such as solvent evaporation, require that the encapsulant is first loaded into a lipid soluble carrier and can be advantageous when using heat-labile molecules [10]. A drawback for chemical homogenization is that they require further processing (ultrafiltration or freeze-drying) and may leave residual organic solvents in the finished emulsions [10].

Mechanical methods such as high shear mixers, microfluidizers, high pressure homogenizers, or ultrasound generators are also used to disperse oil to into water [11]. Because fine emulsion techniques generate a large amount of force on a small amount of volume, a coarse homogenization step (e.g., treatment by a high shear mixer) is used to roughly incorporate the dispersed phase in the continuous phase. The coarse emulsion can then be passed through a fine homogenization step, such as high-pressure homogenization. High-pressure homogenizers work by forcing liquid through small openings, which is controlled by a valve. As the liquid travels through the opening, larger particles are disrupted. Forces are that the liquid experiences are either caused by cavitation or turbulent forces, which tear larger particles into smaller ones [12]. Further heat and mechanical treatment of emulsions can further break apart existing particles to

form smaller particles [13]. While these mechanical means may be costly because of the energy input needed, they do not require the need of organic solvents.

Emulsions can be characterized in many ways. Two measures of emulsions are the particle size and zeta potential. The particle size of emulsion can be used to distinguish emulsions. Emulsions with a particle size of 200 nm-200 μm in diameter are often considered emulsions while emulsion that are 20-200 nm in diameter are often considered as nanoemulsions [14]. Although other definitions for the diameter range of nanoemulsions exist, e.g., 100-250 nm in diameter [15]. The particle size distribution of an emulsion can be reported as a single value, e.g., volume-surface mean (d_{32}) of diameter [4].

On the other hand, zeta potential is the force between two surfaces in a liquid. Zeta potential is described as the "distance away from the droplet surface below which the counter-ions remain strongly attached to the droplet when it moves in an electric field" [4]. The polar moiety of the surfactant is often charged. Because the polar regions of surfactants are by and large the only portion of the emulsion to interact with the continuous phase, the zeta potential of the particle is largely dependent on the polar region of the surfactant. For example, n-tetradecane emulsions made with an anionic surfactant (sodium dodecyl sulfate) or a cationic surfactant (dodecyl trimethylammonium bromide) have negative and positive zeta potentials, respectfully [16]. In general, the higher the absolute value of the zeta potential, the more stable the emulsion because of the repulsion between like-charged particles. Emulsions stabilized with protein will have a negative zeta potential above their isoelectric point and a positive zeta potential below their isoelectric point [4]. Proteins are able to stabilize water and oil because polar and nonpolar amino will tend to associate water and oil environments, respectively. This has been described as a train-loop-tail model [17].

In a thorough review of delivery systems for bioactive lipophilic components, McClements et al. outline roles needed for edible emulsions to fill to be used in the food industry need to:

- be convenient to incorporate into food stuffs when loaded with the encapsulant,
- be inert—not affect the shelf life, texture, flavor, or appearance of the food,
- be a barrier of the encapsulant during the life of the product (with potential of controlled destabilization),
- be simple to process and be made of food-grade components [4].

Depending on the processing conditions the size of the emulsions created can be changed. Nanoemulsions are of interest because they can be made sufficiently small will appear as a transparent or opaque liquid [14] and also have improved stability to separation by gravitational separation and Ostwald ripening [11,18]. Additionally, because of the increased surface area, nanoemulsions are expected to improve the bioavailability of their encapsulants [5].

A major drawback for emulsions is that they are thermodynamically unstable systems. One pathway of instability is by flocculation and coalescence. Flocculation can either be caused by excess surfactant is present in the continuous phase, the results flocs can undergo coalescence where they combine into a larger particle [19]. Another instability pathway is by Ostwald ripening, where molecules from the dispersed phase migrate from small particles to larger ones through the continuous phase [18]. Both instability mechanisms can be followed by tracking the particle size of emulsion particles over time. Particle that increase in size sufficient to separate by the gravity will rise to the top of the liquid or cream [19]. Because nanoemulsions are sufficiently small, Brownian motion overcomes separation by gravity [18].

Because emulsions often have a charged substance at their surface, charged molecules (e.g., pectin or chitosan) can be adsorbed to the surface. Also regarded as layer-by-layer electrostatic deposition technique, this process can be used to increase the size of the interfacial region [20]. A drawback to this technique is the adsorption of uncovered regions of the core emulsion, this is known as bridging flocculation [20]. The addition of polyelectrolyte will change the overall zeta potential of the emulsion droplet to that of the polyelectrolyte [21].

Unfortunately, encapsulants in nanoemulsions are lose their encapsulants through short diffusion pathways; without further medication they have limited application in controlled release [22]. Because liquid emulsion droplets cannot control their encapsulants diffusion, a later approach looked into immobilizing encapsulants into a solid lipid matrix. Because some lipids have melting points high enough to be liquid at room or refrigerated temperatures yet low enough to melt during thermal processing, e.g., hot homogenization, there was an idea of incorporating bioactive molecules directly into the dispersion, where the encapsulant would be uniformly distributed throughout the dispersion [23]. This technique that was proposed is solid lipid nano particles (SLN), where encapsulants are encapsulated into a solid dispersed phase [23]. The determining factor for the dispersed phase of SLN is solid at ca. 37°C. SLN have been formulated using solid materials such as glyceryl dibehenate (Compritol) [24], palmitic or steric acids [25]. These are produced by using a hot melt homogenization technique as temperature sufficient to melt the solid lipid material. Food ingredients such as hydrogenated palm oil and cocoa butter have also been used to formulate SLN [26]. SLN have also been loaded with drugs such as nicotine [25] and rapamycin [27]. In some cases, SLN could be loaded with up 50% of the lipid fraction being an encapsulant while forming a solid dispersion [2]. These have also been used in food applications, e.g. β-carotene [26] and limonene [28]. Because encapsulants would

associate with the dispersed phase of the SLN, they were expected to form a homogenously distributed particles. The next step was to understand the release kinetics of SLN.

This attribute of burst expulsion is a large shortcoming for SLN *per se* and limits their application for controlled release. Qian et al. were interested in comparing the stability of β-carotene from SLN in liquid lipid emulsions (LLN) and SLN [26]. There was a significant change in color of the SLN, which they attribute to expulsion of β-carotene from the structure as the lipids recrystallized [26]. Using an EPR technique, Yucel et al. came to the same result, that the solid component of SLN excludes encapsulants from the dispersed phase of the mixture [22].

Because the solid lipid matrix did effectively exclude encapsulants from the core of SLN, a technique where a liquid core is surrounded by solid particles was proposed in Pickering emulsions [9]. Pickering emulsions overcome the burst release because the lipid core cannot expel carried molecule from the emulsion because of polymorphic transitions. They have good physical stability because the solid particles have shown resistance to coalescence [29]. These have been used in food science applications and have potential for delivery of encapsulants in food applications [30]. Pickering emulsions have also been made of colloidal lipid particles, i.e., tripalmitin as the dispersed phase, by using a similar hot melt homogenization technique, but allowing the homogenizer to cool, crystallizing the tripalmitin during the homogenization [31]. Structures with potential for pH switchable release have been developed with protein-stabilized Pickering emulsions have been formed with caseinate particles [32]. Changing the pH about the isoelectric point of the caseinate-stabilized Pickering emulsions would destabilize the particles which would release the encapsulant.

1.3. Nanostructured lipid systems

The surface properties of emulsion can be customized to alter their characteristics. One alteration is the addition of charged biopolymers which can be adsorbed to an oppositely charged emulsion's surface. This addition can stabilize the emulsion can be deposited onto the emulsion's surface (increasing the size of the interfacial region). This technique can be combined to form Pickering-like structures, made of oppositely charge emulsions [33].

Colloidosomes are an attractive candidate for selective transport of encapsulated ingredients. Colloidosomes use a Pickering emulsion-like mechanism is that they are structures consisting of a core particle which has shell particles self-assembled to its surface. Self-assembly is described as "the autonomous organization of components into patterns or structures without human intervention" [34]. For the case of colloidosomes with emulsions as the core particle, latex has been adsorbed to emulsion surfaces [35] and oppositely charged emulsions [33] have been mixed to form colloidosomes. While the term colloidosome was first given to the structures by Dinsmore et al. (2002) because of the similar of the exterior particles to the phospholipid bilayer of liposomes, similar structures have been previously described by Velev et al first formed hollow latex balls [36] and quickly thereafter formed colloidal aggregate structures [37] which closely resemble colloidosomes.

Because colloidosomes are formed by mixing oppositely charged particles, consideration to the size of both the core and shell particles. Properties of both particles, e.g. particle size and zeta potential, are important factors which will affect the final colloidosomes. Yates et al., were interested in how different particle size ratios of core and shell material affected heteroaggregation of positively charged alumina particles and negatively charged silica particles from a ratio of about 1:70 to about 1:1 (small: large) particles [38]. They found that at lesser

ratios, where the shell material is too small, bridging flocculation can occur [38]. Therefore, the shell material should be sufficiently large to prevent bridging flocculation covered droplets.

While researchers initially used inorganic compounds for the shell material, there is an interest in forming colloidosomes with oppositely charged food-grade emulsions. Because proteins switch their surface charge when crossing about their isoelectric point, proteins are an attractive candidate for creating food-grade colloidosomes. To this point, Gu et al. used whey protein to create colloidosomes from large (ca d_{32} = 600 nm) and small (ca. d_{32} = 200 nm) emulsion particles; where the small particles were pectin was added as a coating to the large particles [33]. When mixing oppositely charged emulsions, they observed that as shell particles are added to large particles, the particle size sees a sharp initial increase in the observed particle size (which they attribute to self-assembly of the oppositely charged particles) and then a decreasing particle size as the small droplet fraction increases [33]. This is graphically depicted in Figure 1.1.

The ratio of shell particles and core particles is another important consideration in designed colloidosomes from emulsions. To form colloidosomes, oppositely charged emulsions have been mixed at different volumetric ratios of core emulsions with shell emulsions [20] and SLN [39]. With an insufficient amount shell particles, bridging flocculation occurs between partially covered core particles [40]. Whereas at superfluous amounts of shell material, depletion flocculation can occur, where attractive forces overcome repulsive forces [40].

Colloidosomes are composed of a core particle surrounded by shell particles, it may be intuitive to think that the particle size of the exterior particles would affect the rate of transport from the core particle. Transport of aspirin and caffeine from the core particle was not related to the particle size of the shell particles [41]. As the volume available for transport decreases the

tortuosity of flow through the gap [42]. Rosenberg and Dan attribute the rate of diffusion to the thickness of the shell, because the thickness of the shell only equals the particle size of the shell particles in monodisperse colloidosomes, they propose to use two particle sizes of shell particles to reduce transport from the core particle [43].

Further treatment of colloidosomes is possible, this can be advantageous because of the pores created by the addition of the shell material will allow some diffusion. Colloidosomes made of a span 80 liquid lipid emulsion surrounded by poly(styrene-co-butyl-acrylate) were loaded with a fluorescent dye and sintered for various amounts of time [44]. In this study, Yow and Routh found that when their colloidosomes were sintered for 60 min at 49°C, the release of the fluorescent dye was reduced considerably [44]. Another approach is to cross-link the shell particles. Although Thompson et al., conclude that cross-linked colloidosomes failed to slow the release of the fluorescent dye [45].

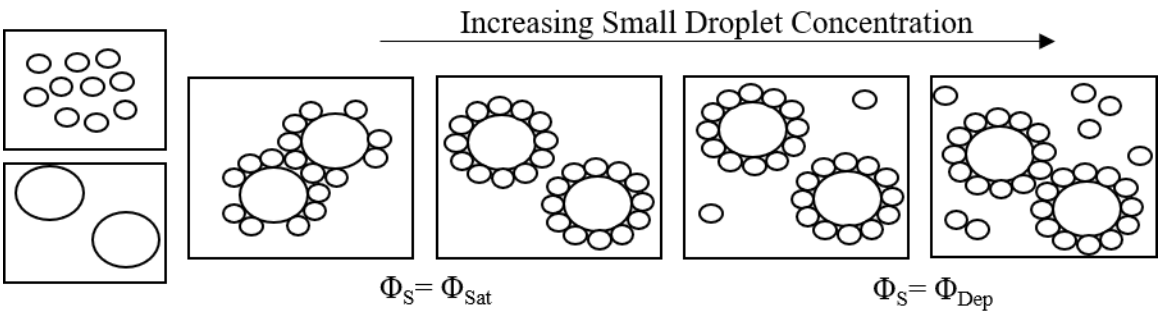

Figure 1.1. Schematic representation of self-assembly of large anionic droplets to small cationic droplets where Φ_S is the volumetric fraction of small particles, Φ_{Sat} is the volumetric fraction of small particles which saturates the large particles, and Φ_{Dep} is the volumetric fraction of small particles where depletion flocculation occurs (Adapted from [33]**).**

1.4. Liposomal vesicles

Liposomal vesicles (LV) are structures are composed of one of many bilayers. LV first became of interest to scientists because of their resemblance to lipid bilayers in biological systems [46]. Because they are conceptually an attractive delivery systems, LV have been used in the cosmetic field was by Dior, in their product Capture, in 1986 [47]. They have since gained interest in the pharmaceutical interest for their use as stimuli-responsive delivery systems, such as changes in pH or responses to biological processes [48].

LV are often made of phospholipids, many of the physical characteristics of LV can be manipulated by the composition of the phosphate and lipid moieties. For example, the zeta potential of LV is determined by the head group and the rheology, permeability, and solubilization are determined by the fatty acid tail's composition (e.g. chain length and unsaturations) [49].

The charge of the head group on the phospholipid can determine how guest molecules will align in the dispersion [50]. The zeta potential of the liposomes can change with the addition of guest molecules. When drugs were loaded into egg phosphatidylcholine, the overall zeta potential of the formed liposomes became increasingly negative [51]. Which was attributed to the change in orientation of the water-soluble phosphate and choline groups.

Additionally, when guest molecules are incorporated into LV, they can increase the particle size by as much as ca. 30% [50]. Because saturated fatty acid chains are generally linear, it is expected that unsaturated fatty acids would add irregularities, kinks, into the lipid bilayer. Unsaturated fatty acids will have lower transition temperatures (melting or crystallization) [52]. The irregularity in membrane can cause the packing in the membrane to change from lamellar to

hexagonal [53]. The change in lamellarity can destabilize the structure of the lipid region, which in turn would expel the encapsulant [48].

There is great potential for use of LV for the delivery of small molecules because of their high surface area with potential to be made much smaller than the wavelength of visible light [49]. LV can associate into single or multiple bilayers (Figure 1.2). These are divided into subcategories which are named by their lamellarity: small unilamellar vesicles (SUV), large unilamellar vesicles (LUV), multilamellar liposomal vesicles (MLV) are composed of multiple bilayers, or multivesicular vesicles (MVV). Liposomes can be prepared in methods similar to emulsions. The use of high energy homogenization techniques (e.g., high pressure homogenization) typically produces SUV while lower energy methods will produce MLV and MVV [15]. This is because phospholipids are amphiphilic by nature and will self-associate in the less organized MLV and MVV structures without additionally energy to decrease the particle size. Conventional methods to produce MLV and MVV typically create structures that are 200 nm in diameter or greater [54]. On the other hand, because SUV require high energy input they can be made at smaller dimensions.

The packing fatty acid tails of LV determine the permeability of the delivery system. Because phospholipids can have long fatty acids tails, the state of the tail can become crystalline, which decreases the hydrophobic interacts within the lipid bilayer [55]. The enthalpy change, measured by differential scanning calorimetry (DSC), can be used to determine the state of the liposome membrane [55]. The addition of longer saturated fatty acids will make LV less permeable while having shorter unsaturated fatty acids will make LV more permeable [49]. The membrane behavior can also be modulated by the addition of carrier lipids, such as cholesterol,

to make the barrier more rigid. The incorporation of the carrier lipid into the LV membrane can be observed as a decrease in the onset temperature and enthalpy of the crystallization peak [56].

The addition of encapsulants also affects the ability to encapsulate other molecules. These guest molecules interfere with the fatty acid tails of the lecithins. Liposomes can be loaded with guest molecules, e.g., flavors or antioxidants, in a passive or active loading technique. The passive loading method is done by simply empty prepared, empty, liposomes with the desired guest molecule. Hydrophobic guest molecules will incorporate into the lipid bilayer [49]. On the other hand, an active loading technique loads liposomes by mass transfer of weak acids or bases into the lipid bilayers; the uncharged fraction of the acid or base associates in liposome lipid bilayer [49]. For both method as the fraction of guest molecules increases, the overall particle size of the liposomes also increases [57].

Additionally, empty liposomes can be present after the homogenization step [57]. The presence of empty liposomes could affect the interpretation of liposomes loaded with small molecules. Because the incorporation of guest molecules into liposomes increases the particle, energy intensive processes may need to be sufficiently investigated to ensure the incorporation of the molecules of interest into the LV structure, such as DSC [56].

One drawback to LV in practice is that they have complicated and expensive quality assurance testing, e.g. electron microscopy [23]. Further, McClements describes some additional limitations of LV to be difficulty making them consistently, limited stability in typical food environments, and poor encapsulation efficiency of water-soluble bioactive molecules in the loading stage [49]. There is a need to understand how guest molecules, such as bioactive compounds, are incorporated into LV and how diffusion from LV changes with increasing guest molecule concentration.

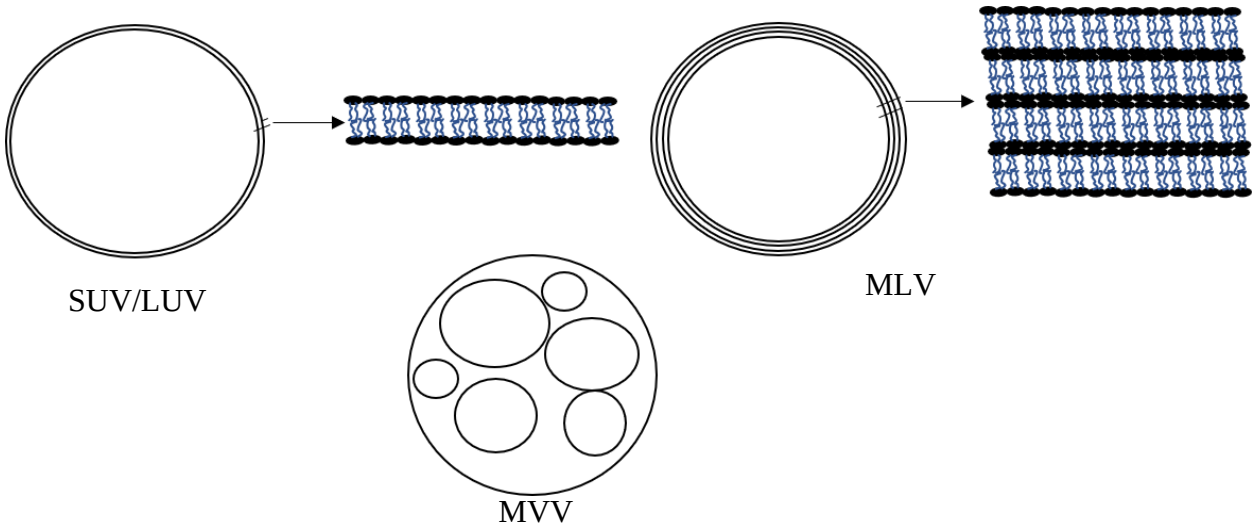

Figure 1.2. Small or large unilamellar vesicles (SUV/LUV), multilamellar vesicles (MLV), and multivesicular vesicles (MVV). Adapted from [46]**.**

1.5. Characterization

1.5.1. Physical characterization

To measure particle size of emulsions can be measured by a variety of techniques. Light scattering techniques such as static light scattering [58], dynamic light scattering [20], and small angle x-ray scattering (SAXS) [59] can be used to measure the particle size of dispersions in liquids. Static light scattering is based on the refraction of light that passes through a liquid with particles and dynamic light scattering is based on the Brownian movement of particles in a liquid, and (SAXS) is based on diffraction at various angles. Other techniques are available to measure particle size of dispersions in liquids, such as back scattering [60] (which may not penetrate into the sample enough to collect a representative measurement), ultrasound spectrometry [61] (although no method has been established for ultrasonic determination of particle size), and microscopy techniques (which may be inefficient to collect a sufficiently large sample size for an accurate measurement)[50] can be used to measure the particle size. While backscattering does not require a dilution of the dispersion, light scattering techniques typically need a dilution to avoid multiple scattering effects, where the light source interacts with multiple particles in the dispersion [61]. On the other hand, backscattering and ultrasonic techniques can be made on more concentrated systems [61]. Additionally, an advantage of using DLS is that it can be used to measure zeta potential at the same time as particle size.

With the use of many phases in delivery systems, there is a need to understand the physical state of components in delivery systems. Physical methods are able to give information about the system. One such physical method is differential scanning calorimetry (DSC). Because DSC monitors the heat flow as a function of temperature, it can provide information to phase

transitions of solid lipids used in delivery systems, e.g., phase transitions of the solid component of a SLN [23]. DSC has been used to investigate the packing of fatty acids in liposomal vesicles or drugs incorporated into the lipid bilayer [55]. DSC has also been used to mass transfer of solid lipids from SLN in the presence of SLN [63]. Additionally, low resolution nuclear magnetic resonance (NMR) spectroscopy can be used to characterize the solid fat content in an emulsion [63].

1.5.2. Zeta potential

The zeta potential is a measure of the electrical charge on exterior of a particle, or the Stern layer [62], and the shear plane [4]. Zeta potential can be measured using the theory developed by Derjaguin and Landau, and separately by Verwey and Overbeek, or DLVO theory. This theory considers attractive forces (Van der Waals attraction) and repulsive forces (electrostatic repulsion) to estimate the electrical charge on a surface [62]. This is a useful measurement for colloidal dispersions because it can be used as a measure of stability. It can be calculated at the same time as some particle size analysis (dynamic light scattering) by measuring shifts in shift of particles in an applied electrical field. Particles with a high absolute value zeta potential will tend to repel from particles with the same charge [4].

1.5.3. Small molecule behavior

Work is needed in understanding the distribution of small molecules in their delivery systems. A simple method is to measure the absorbance of a known wavelength is by UV-Vis spectrophotometry, because many molecules of interest in food applications have bands that will absorb on the UV-Vis range such as curcumin. To measure of curcumin in Pickering emulsions, UV-Vis was been used to measure the amount of curcumin was present in the create Pickering

emulsions throughout a simulated digestion [30]. In this case, UV-Vis is a simple method for quantifying the encapsulant in both the continuous and oil phases of the emulsion However, a drawback here is that the method used was destructive to the emulsions used in the study, by adding methanol to extract encapsulated curcumin. Alternatively, a nondestructive method is color analysis. To study β-carotene in SLN, Qian et al. used a colorimetric method was to measure the color of β-carotene in SLN and a similar liquid emulsion (2013). In this study, the color change is used to indicate the stability of β-carotene, as the emulsions they study age [26]. Two limitations of using color to study encapsulants in emulsions are that they only observe the continuous phase or at the emulsions surface and that measurements are only meaningful of systems loaded with colorful samples. While these methods simple, they are limited because they provide information about the system as a whole, which does not provide information about what is released.

A class of methods uses to study volatile molecules is by measuring the headspace above an emulsion. One method is by gas chromatography-mass spectroscopy (GC-MS), which is able to look at the headspace above a food or emulsion. Ghosh et al. estimated the concentration flavor molecules by measuring the concentration of those molecules in the headspace using both the oil-water and air-water log *P* values for oil [64]. A drawback to this method is that GC-MS only works on volatile molecules. GC-MS also cannot be used for continuous monitoring of a sample.

Atmospheric pressure chemical ionization mass spectroscopy (APcI-MS) is a similar method have been used to quantify the concentration of flavor molecules from headspace above a delivery system or directly from the breath of a human who is consuming a product. APcI-MS is often used as the detector for liquid chromatography scheme. Without the use of a separation

scheme, APcI can be used to continuously detect volatile compounds in the headspace above a sample, allowing for analysis in real time. Compared to GC-MS, APcI allows for the continual monitoring above the sample. APcI-MS can also be used to study larger molecules by incorporating tandem MS [65]. APcI-MS has been used to quantify flavor compounds in hard candy [66] and chewing gum [67]. The APcI-MS method can be advantageous for monitoring the concentration of volatiles during consumption, although another method would be needed to discover concentration in the delivery system.

Magnetic resonance techniques are noninvasive and can provide information regarding dynamic phenomena, such as release profiles of emulsions [23]. Nuclear magnetic resonance (NMR) spectroscopy is a technique that is able to determine physical characteristics of dispersions. Low resolution NMR has been used to monitor mass transfer of solid palm stearin from SLN in the presence of liquid oil emulsions, based on the solid fat content of the SLN [63]. Bonechi et al., used high-resolution one-dimensional H-NMR to investigate the distribution of *trans*-resveratrol in zwitterionic and cationic liposomes [50]. Further, they also use two-dimensional NMR (NOESY) to locate encapsulated resveratrol in liposomes, based on the interaction of the hydrogens in resveratrol interacting with the hydrogens in the phospholipid [50].

1.6. Electron paramagnetic resonance spectroscopy

1.6.1. Principles

One method to follow distribution of small molecules in dispersions is with EPR. This method first became popular when microwaves gained widespread popularity following World War II [68]. EPR spectroscopy is a form of magnetic resonance spectroscopy that is based on the

magnetic moments of paramagnetic species, i.e., free radicals [68]. Spin of free radicals are random without the addition of an external force. When a magnetic field is applied to those free radicals, the magnetic mobility of free radicals is limited, which causes a change in the energy level of the electron [68]. The transition between the two energy levels of the confined electrons in a magnetic field follows Planck's law, resulting in the absorption of upper (+) and lower (-) electromagnetic energy [68]. The energy difference between the upper and lower states (ΔE) can be described by Eq. 1:

$$\Delta E = h\nu = g\mu_B B_0 \qquad \text{[Eq. 1]}$$

Where h is Planck's constant, ν is the frequency of electromagnetic radiation, g is the g-factor, μ_B is the Bohr Magneton, and B_0 is the magnetic field strength [69].

EPR spectra are created by changing magnetic field strength at a constant frequency, free radicals will orient in low and high energy fields [68]. When the magnetic field strength equals the energy difference between the two states, the maximum energy absorption occurs, which is determined by the g-factor of the sample [68]. When free radicals interact with neighboring nuclei in the magnetic field, they will produce splits in the spectra, the difference is called hyperfine splitting (a_N) [68]. The a_N is based on the quantum spin number (I) of the nucleus of the atom; the effective quantum spin number of ^{14}N is I = 1 (Fig. 3) [69].

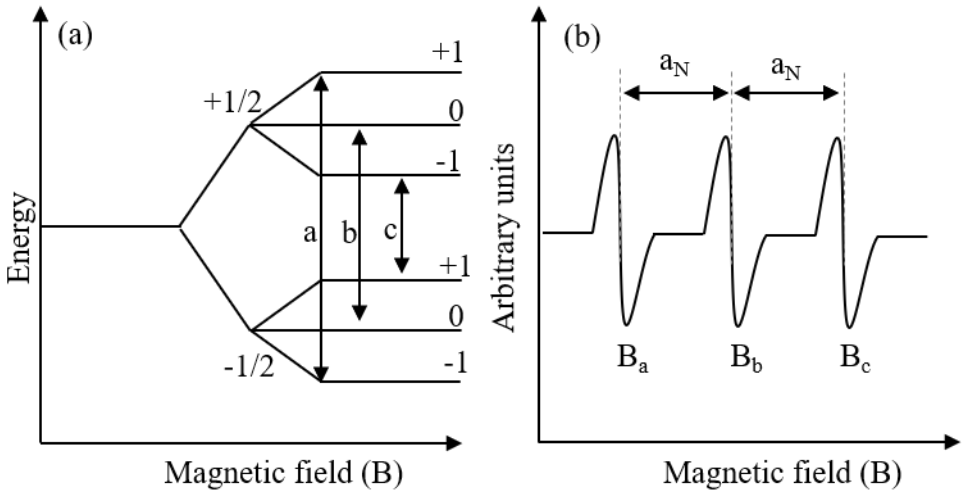

Figure 1.3. (a) Scheme of energy of an atom bearing a free radical with a quantum spin number of (I = 1) as a function of magnetic field strength and (b) an EPR sketch of the same atom. Adapted from [68]**.**

1.6.2. Food applications

EPR has been used to characterize oxidation prone foods and beverages, because they often contain oxidizing agents (e.g., transition metal, ascorbate, or sulfite ions) and can have oxygen incorporated into them. EPR spin trapping, i.e., compounds that form stable nitroxide radicals after reacting with free radicals from the environment, has been used to measure oxidation in beverages. When studying oxidative stress in beer spin traps can be used to investigate the formation of hydroxyl radicals in the early stages of the fermentation process [70]. This reaction is a Fenton-like reaction where oxidizing agents, often ferrous iron in foods, oxidize hydrogen peroxide, which produces a free hydroxyl ion and a hydroxyl radical [70]. EPR spin trapping has been used in wine to further understand mechanisms of failure [71]. A similar method has been used to track the formation and decline of free electrons in coffee after brewing [72] and understanding the impact of reactivity of polyphenols in model food systems [1].

1.6.3. Characterization of distribution

EPR can also be used to characterize the membranes of delivery systems (e.g., liposomes and emulsions) and the distribution of molecules. Although this method requires an EPR-active compound (spin probe) to be added to the dispersion, it is nondestructive a nondestructive technique. A variety of nitroxide radicals are commercially available, it is possible to select a spin probe that will partition between phases of interest.

EPR spin probes have been used to investigate the structure of membranes. This can be done with the order parameter, which is a scale of randomness of a spin probe within a a membrane. Both 5- and 16-doxyl-stearic acids (5-DSA and 16-DSA, respectively) have been used to characterize the order within liposome membranes, such as carotenoids [73]. Because both of these ingredients will favor environments with different polarities, the more polar 5-DSA can be used as a measure of the membrane interface with the more polar phase and the less polar 16-DSA can be used as a measure of the nonpolar environment. Because the order parameter gives information about the physical state of the bilayer, it may be used to understand the effect guest molecules have on lipid bilayers of liposomes. Indeed, 5-DSA and 16-DSA have been loaded into liposomes to investigate the effect unsaturated fatty acids have on liposome permeability [54]. This has also been used to characterize membrane structures of microorganisms, such as *Escherichia coli* [74].

One such spin probe is 4-phenyl-2,2,5,5-tetramethyl-3-imidazoline-1-oxyl nitroxide (PTMIO), which has been used to study distribution in emulsions [22,75,76]. Because PTMIO has a log *P* value of 2.5, it will largely associate in the hydrophobic region of emulsions. EPR gives insight to the microviscosity and micropolarity of the spin probe [23]. EPR spectra will provide insight into the mobility of the paramagnetic species in that environment. A nitroxide

radical will have a triplet EPR spectrum, a mobile nitroxide radical will display three narrow peaks; on the other hand, PTMIO in liposomes will appear in the spectra by the presence of peaks with distinct a_N from the high and low field peaks of spin probes that are located within a membrane [2]. Comparing spin probes of different log *P* values in emulsions, Carabin et al. showed that the hydrophilic spin probe 4-hydroxy-2,2,6,6-tetramethylpiperidine 1-oxyl (TEMPOL) was only present in the aqueous phase, PTMIO partitioned between the two phases, and 16-DSA was only located in the emulsion core [77].

Complex EPR spectra can be further processed by deconvolution to separate fractions of spin probes in distinct microenvironments. Simulations software can be used to separate fractions of spin probes in distinct environments because fractions in different environments with a distinct polarity will also have a distinct a_N [75]. One method to deconvolute complex EPR spectra is by using software to run a downhill simplex to separate fractions of spin probes with unique a_N. Deconvolution has been used to separate fractions of spin probes in aqueous phase and at within the phospholipid layer of SLN [78]. Simulation of PTMIO-containing emulsions and micelles was used to understand the location and reactivity of the model hydrophobic ingredient [22].

Moreover, an ascorbate assay of a spin probe provides the ability to track reaction progress in real time [75]. EPR used in conjunction with an ascorbate assay allows for insights into the distribution of model hydrophobic ingredients *in-situ.* This has been used to study the location of PTMIO during ascorbate reactions in an emulsion in real time, finding that the rate of PTMIO diffusion is greater than the rate of ascorbate reduction in the aqueous phase [22]. Because ascorbate is largely polar, the reduction of PTMIO is expected to happen in the aqueous phase. In comparing the reactivity of spin probes with different polarities in emulsions, the

argument that water soluble TEMPOL reacts more quickly with ascorbate than spin probes that associate in the lipid core of emulsions [77]. Because deconvolution of complex EPR spectra provides insights into molecules in distinct environments, simulation of EPR spectra during an ascorbate assay can provide information as to which fraction of a spin probe is reacting with the water-soluble ascorbate. Simulation of PTMIO reduction kinetics has been used to understand the distribution of hydrophobic ingredients in SLN [22]. Yucel et al. found that PTMIO was effectively excluded from SLN, which they attribute to the transition between polymorphic structures of the solid lipid in the dispersed phase [22]. Although, when the highly lipid soluble 16-DSA was exposed to an ascorbate reaction in a liquid emulsion and SLN, 16-DSA's reactivity was not affected by the state of the lipid core whereas PTMIO was degraded more quickly in SLN [77].

1.7. References

[1] L. Zhou, R.J. Elias, Factors influencing the antioxidant and pro-oxidant activity of polyphenols in oil-in-water emulsions, J. Agric. Food Chem. 60 (2012) 2906–2915. doi:10.1021/jf204939h.

[2] G. Martini, L. Ciani, Electron spin resonance spectroscopy in drug delivery, Phys. Chem. Chem. Phys. 11 (2009) 211–254. doi:10.1039/b808263d.

[3] IUPAC, Compendium of Chemical Terminology, 2nd ed. (t, Blackwell Scientific Publications, Oxford, 1997. doi:https://doi.org/10.1351/goldbook.

[4] D.J. McClements, E.A. Decker, J. Weiss, Emulsion-based delivery systems for lipophilic bioactive components, J. Food Sci. 72 (2007). doi:10.1111/j.1750-3841.2007.00507.x.

[5] E. Acosta, Bioavailability of nanoparticles in nutrient and nutraceutical delivery, Curr. Opin. Colloid Interface Sci. 14 (2009) 3–15. doi:10.1016/j.cocis.2008.01.002.

[6] L. Salvia-Trujillo, C. Qian, O. Martín-Belloso, D.J. McClements, Influence of particle size on lipid digestion and β-carotene bioaccessibility in emulsions and nanoemulsions, Food Chem. 141 (2013) 1472–1480. doi:10.1016/J.FOODCHEM.2013.03.050.

[7] F. Donsì, M. Sessa, H. Mediouni, A. Mgaidi, G. Ferrari, Encapsulation of bioactive compounds in nanoemulsion- based delivery systems, Procedia Food Sci. 1 (2011) 1666–1671. doi:10.1016/j.profoo.2011.09.246.

[8] J. Genova, H. Chamati, Z. Slavkova, M. Petrov, Differential Scanning Calorimetric Study of the Effect of Cholesterol on the Thermotropic Phase Behavior of the Phospholipid 1-Stearoyl-2-Oleoyl-sn-Glycero-3-Phosphocholine, J. Surfactants Deterg. (2019) 516–522.

doi:10.1002/jsde.12289.

[9] S.U. Pickering, CXCVI.-- Emulsions., (1906) 2001–2021.

[10] M.A. Iqbal, S. Md, J.K. Sahni, S. Baboota, S. Dang, J. Ali, Nanostructured lipid carriers system: Recent advances in drug delivery, J. Drug Target. 20 (2012) 813–830. doi:10.3109/1061186X.2012.716845.

[11] T. Tadros, P. Izquierdo, J. Esquena, C. Solans, Formation and stability of nano-emulsions, Adv. Colloid Interface Sci. 108–109 (2004) 303–318. doi:10.1016/j.cis.2003.10.023.

[12] S. Schultz, G. Wagner, K. Urban, J. Ulrich, High-pressure homogenization as a process for emulsion formation, Chem. Eng. Technol. 27 (2004) 361–368. doi:10.1002/ceat.200406111.

[13] J. Rao, D.J. McClements, Formation of flavor oil microemulsions, nanoemulsions and emulsions: Influence of composition and preparation method, J. Agric. Food Chem. 59 (2011) 5026–5035. doi:10.1021/jf200094m.

[14] D.J. McClements, Edible nanoemulsions: Fabrication, properties, and functional performance, Soft Matter. 7 (2011) 2297–2316. doi:10.1039/c0sm00549e.

[15] I.J. Joye, G. Davidov-Pardo, D.J. McClements, Nanotechnology for increased micronutrient bioavailability, Trends Food Sci. Technol. 40 (2014) 168–182. doi:10.1016/j.tifs.2014.08.006.

[16] C.C. Berton-Carabin, R.J. Elias, J.N. Coupland, Reactivity of a model lipophilic ingredient in surfactant-stabilized emulsions: Effect of droplet surface charge and

ingredient location, Colloids Surfaces A Physicochem. Eng. Asp. 418 (2013) 68–75. doi:10.1016/j.colsurfa.2012.11.010.

[17] E. Dickinson, Caseins in emulsions: Interfacial properties and interactions, Int. Dairy J. 9 (1999) 305–312. doi:10.1016/S0958-6946(99)00079-5.

[18] T.J. Wooster, M. Golding, P. Sanguansri, Ripening Stability, Langmuir. 24 (2008) 12758–12765. doi:10.1021/la801685v.

[19] E. Dickinson, Flocculation of protein-stabilized oil-in-water emulsions, Colloids Surfaces B Biointerfaces. 81 (2010) 130–140. doi:10.1016/j.colsurfb.2010.06.033.

[20] D. Guzey, D.J. McClements, Formation, stability and properties of multilayer emulsions for application in the food industry, Adv. Colloid Interface Sci. 128–130 (2006) 227–248. doi:10.1016/j.cis.2006.11.021.

[21] K.G. Zinoviadou, E. Scholten, T. Moschakis, C.G. Biliaderis, Properties of emulsions stabilised by sodium caseinate-chitosan complexes, Int. Dairy J. 26 (2012) 94–101. doi:10.1016/j.idairyj.2012.01.007.

[22] U. Yucel, R.J. Elias, J.N. Coupland, Solute distribution and stability in emulsion-based delivery systems: An EPR study, J. Colloid Interface Sci. 377 (2012) 105–113. doi:10.1016/J.JCIS.2012.03.071.

[23] R.H. Müller, K. Mader, S. Gohla, Solid lipid nanoparticles (SLN) for controlled drug delivery - review of the state of the art, Eur. J. Pharm. Biopharm. 50 (2000) 161–177. doi:10.1016/s0928-0987(97)86243-4.

[24] J. Mazuryk, T. Deptuła, A. Polchi, J. Gapiński, S. Giovagnoli, A. Magini, C. Emiliani, J.

Kohlbrecher, A. Patkowski, Rapamycin-loaded solid lipid nanoparticles: Morphology and impact of the drug loading on the phase transition between lipid polymorphs, Colloids Surfaces A Physicochem. Eng. Asp. 502 (2016) 54–65. doi:10.1016/j.colsurfa.2016.05.017.

[25] Y. Ding, K.A. Nielsen, B.P. Nielsen, N.W. Bøje, R.H. Müller, S.M. Pyo, Lipid-drug-conjugate (LDC) solid lipid nanoparticles (SLN) for the delivery of nicotine to the oral cavity – Optimization of nicotine loading efficiency, Eur. J. Pharm. Biopharm. 128 (2018) 10–17. doi:10.1016/j.ejpb.2018.03.004.

[26] C. Qian, E.A. Decker, H. Xiao, D.J. McClements, Impact of lipid nanoparticle physical state on particle aggregation and β-carotene degradation: Potential limitations of solid lipid nanoparticles, Food Res. Int. 52 (2013) 342–349. doi:10.1016/j.foodres.2013.03.035.

[27] K.E. Preece, N. Hooshyar, A. Krijgsman, P.J. Fryer, N.J. Zuidam, Intensified soy protein extraction by ultrasound, Chem. Eng. Process. - Process Intensif. 113 (2017) 94–101. doi:10.1016/j.cep.2016.09.003.

[28] V. Trinetta, M.T. Morgan, J.N. Coupland, U. Yucel, Essential oils against pathogen and spoilage microorganisms of fruit juices: use of versatile antimicrobial delivery systems, J. Food Sci. 82 (2017) 471–476. doi:10.1111/1750-3841.13614.

[29] A.B. Pawar, M. Caggioni, R. Ergun, R.W. Hartel, P.T. Spicer, Arrested coalescence in Pickering emulsions, Soft Matter. 7 (2011) 7710–7716. doi:10.1039/c1sm05457k.

[30] R. V. Tikekar, Y. Pan, N. Nitin, Fate of curcumin encapsulated in silica nanoparticle stabilized Pickering emulsion during storage and simulated digestion, Food Res. Int. 51

(2013) 370–377. doi:10.1016/J.FOODRES.2012.12.027.

[31] A. Schröder, J. Sprakel, K. Schroën, J.N. Spaen, C.C. Berton-Carabin, Coalescence stability of Pickering emulsions produced with lipid particles: A microfluidic study, J. Food Eng. 234 (2018) 63–72. doi:10.1016/J.JFOODENG.2018.04.007.

[32] M. Sarker, N. Tomczak, S. Lim, Protein Nanocage as a pH-Switchable Pickering Emulsifier, ACS Appl. Mater. Interfaces. 9 (2017) 11193–11201. doi:10.1021/acsami.6b14349.

[33] Y.-S. Gu, E.A. Decker, D.J. McClements, Formation of colloidosomes by adsorption of small charged oil droplets onto the surface of large oppositely charged oil droplets, Food Hydrocoll. 21 (2007) 516–526. doi:10.1016/J.FOODHYD.2006.05.011.

[34] G.M. Whitesides, B. Grzybowski, Self-assembly at all scales, Science (80-.). 295 (2002) 2418–2421. doi:10.1126/science.1070821.

[35] A.D. Dinsmore, M.F. Hsu, M.G. Nikolaides, M. Marquez, et al, Colloidosomes: Selectively permeable capsules composed of colloidal particles, Sci. Washingt. 298 (2002) 1006–9.

[36] O.D. Velev, K. Furusawa, K. Nagayama, Assembly of Latex Particles by Using Emulsion Droplets as Templates. 1. Microstructured Hollow Spheres, Langmuir. 12 (1996) 2374–2384. doi:10.1021/la9506786.

[37] O.D. Velev, K. Furusawa, K. Nagayama, Assembly of latex particles by using emulsion droplets as templates. 1. microstructured hollow spheres, Langmuir. 12 (1996) 2374–2384. doi:10.1021/la9506786.

[38] P.D. Yates, G. V. Franks, S. Biggs, G.J. Jameson, Heteroaggregation with nanoparticles: Effect of particle size ratio on optimum particle dose, Colloids Surfaces A Physicochem. Eng. Asp. 255 (2005) 85–90. doi:10.1016/j.colsurfa.2004.12.035.

[39] H. Salminen, T. Helgason, B. Kristinsson, K. Kristbergsson, J. Weiss, Formation of nanostructured colloidosomes using electrostatic deposition of solid lipid nanoparticles onto an oil droplet interface, Food Res. Int. 79 (2016) 11–18. doi:10.1016/j.foodres.2015.11.031.

[40] D.J. McClements, Theoretical analysis of factors affecting the formation and stability of multilayered colloidal dispersions, Langmuir. 21 (2005) 9777–9785. doi:10.1021/la0512603.

[41] R.T. Rosenberg, N.R. Dan, Controlling surface porosity and release from hydrogels using a colloidal particle coating, J. Colloid Interface Sci. 349 (2010) 498–504. doi:10.1016/j.jcis.2010.05.095.

[42] R.T. Rosenberg, N.R. Dan, Diffusion through colloidosome shells, J. Colloid Interface Sci. 354 (2011) 478–482. doi:10.1016/j.jcis.2010.11.011.

[43] R.T. Rosenberg, N. Dan, Effect of colloidal particle size on adsorbed monodisperse and bidisperse monolayers, Langmuir. 27 (2011) 8729–8734. doi:10.1021/la200732f.

[44] H.N. Yow, A.F. Routh, Release Profiles of Encapsulated Actives from Colloidosomes Sintered for Various Durations, Langmuir. 25 (2009) 159–166. doi:10.1021/la802711y.

[45] K.L. Thompson, S.P. Armes, J.R. Howse, S. Ebbens, I. Ahmad, J.H. Zaidi, D.W. York, J.A. Burdis, Covalently cross-linked colloidosomes, Macromolecules. 43 (2010) 10466–

10474. doi:10.1021/ma102499k.

[46] T.M. Taylor, P.M. Davidson, B.D. Bruce, J. Weiss, Liposomal nanocapsules in food science and agriculture, Crit. Rev. Food Sci. Nutr. 45 (2005) 587–605. doi:10.1080/10408390591001135.

[47] R.H. Müller, M. Radtke, S.A. Wissing, Solid lipid nanoparticles (SLN) and nanostructured lipid carriers (NLC) in cosmetic and dermatological preparations, Adv. Drug Deliv. Rev. 54 (2002) S131–S155. doi:10.1016/S0169-409X(02)00118-7.

[48] Y. Lee, D.H. Thompson, Stimuli-responsive liposomes for drug delivery, Wiley Interdiscip. Rev. Nanomedicine Nanobiotechnology. 9 (2017) e1450. doi:10.1002/wnan.1450.

[49] D.J. McClements, Encapsulation, protection, and release of hydrophilic active components: Potential and limitations of colloidal delivery systems, Adv. Colloid Interface Sci. 219 (2015) 27–53. doi:10.1016/j.cis.2015.02.002.

[50] C. Bonechi, S. Martini, L. Ciani, S. Lamponi, H. Rebmann, C. Rossi, S. Ristori, Using liposomes as carriers for polyphenolic compounds: The case of Trans-resveratrol, PLoS One. 7 (2012). doi:10.1371/journal.pone.0041438.

[51] D.G. Fatouros, S.G. Antimisiaris, Effect of amphiphilic drugs on the stability and zeta-potential of their liposome formulations: A study with prednisolone, diazepam, and griseofulvin, J. Colloid Interface Sci. 251 (2002) 271–277. doi:10.1006/jcis.2002.8432.

[52] B. Maherani, E. Arab-Tehrany, M. R. Mozafari, C. Gaiani, M. Linder, Liposomes: A Review of Manufacturing Techniques and Targeting Strategies, Curr. Nanosci. 7 (2011)

436–452. doi:10.2174/157341311795542453.

[53] G. Candiani, D. Pezzoli, L. Ciani, R. Chiesa, S. Ristori, Bioreducible liposomes for gene delivery: From the formulation to the mechanism of action, PLoS One. 5 (2010) 1–8. doi:10.1371/journal.pone.0013430.

[54] M.A. Vélez, M.C. Perotti, P. Zanel, E.R. Hynes, A.M. Gennaro, Soy PC liposomes as CLA carriers for food applications: Preparation and physicochemical characterization, J. Food Eng. 212 (2017) 174–180. doi:10.1016/j.jfoodeng.2017.06.001.

[55] C. Demetzos, Differential Scanning Calorimetry (DSC): A tool to study the thermal behavior of lipid bilayers and liposomal stability, J. Liposome Res. 18 (2008) 159–173. doi:10.1080/08982100802310261.

[56] C. Matsingou, C. Demetzos, Calorimetric study on the induction of interdigitated phase in hydrated DPPC bilayers by bioactive labdanes and correlation to their liposome stability. The role of chemical structure, Chem. Phys. Lipids. 145 (2007) 45–62. doi:10.1016/j.chemphyslip.2006.10.004.

[57] B. Lohse, P.Y. Bolinger, D. Stamou, Encapsulation efficiency measured on single small unilamellar vesicles, J. Am. Chem. Soc. 130 (2008) 14372–14373. doi:10.1021/ja805030w.

[58] H. Salminen, T. Helgason, B. Kristinsson, K. Kristbergsson, J. Weiss, Formation of solid shell nanoparticles with liquid ω-3 fatty acid core, Food Chem. 141 (2013) 2934–2943. doi:10.1016/j.foodchem.2013.05.120.

[59] J. Wagner, W. Härtl, R. Hempelmann, Characterization of monodisperse colloidal

particles: comparison between SAXS and DLS, Langmuir. 16 (2000) 4080–4085. doi:10.1021/la991125o.

[60] A. Lopez-Rubio, E.P. Gilbert, Neutron scattering: a natural tool for food science and technology research, Trends Food Sci. Technol. 20 (2009) 576–586. doi:10.1016/j.tifs.2009.07.008.

[61] D.J. McClements, Principles of ultrasonic droplet size determination in emulsions, Langmuir. 12 (1996) 3454–3461. doi:10.1021/la960083q.

[62] P. Walstra, Colloidal Interactions, in: Phys. Chem. Foods2, New York, NY, 2004: pp. 455–493.

[63] M. Samtlebe, U. Yucel, J. Weiss, J.N. Coupland, Stability of solid lipid nanoparticles in the presence of liquid oil emulsions, JAOCS, J. Am. Oil Chem. Soc. 89 (2012) 609–617. doi:10.1007/s11746-011-1944-3.

[64] S. Ghosh, D.G. Peterson, J.N. Coupland, Effects of droplet crystallization and melting on the aroma release properties of a model oil-in-water emulsion, J. Agric. Food Chem. 54 (2006) 1829–1837. doi:doi.org/10.1021/jf052262w.

[65] J.S. Smith, R.A. Thakur, Mass spectroscopy, in: S.S. Nielson (Ed.), Food Anal., 4th ed., Springer, New York, NY, 2010: pp. 457–470.

[66] A.L. Schober, D.G. Peterson, Flavor Release and Perception in Hard Candy: Influence of Flavor Compound-Flavor Solvent Interactions, J. Agric. Food Chem. 52 (2004) 2628–2631. doi:10.1021/jf0354287.

[67] S. Raithore, D.G. Peterson, Effects of polyol type and particle size on flavor release in

chewing gum, Food Chem. 253 (2018) 293–299. doi:10.1016/J.FOODCHEM.2018.01.123.

[68] J. Weil, J. Bolton, Electron Paramagnetic Resonance: Elementary Theory and Pracitcal Applications, E1 ed., John Wiley & Sons, Hoboken, NJ, USA, 2006.

[69] S. Kempe, H. Metz, K. Mäder, Application of Electron Paramagnetic Resonance (EPR) spectroscopy and imaging in drug delivery research - Chances and challenges, Eur. J. Pharm. Biopharm. 74 (2010) 55–66. doi:10.1016/j.ejpb.2009.08.007.

[70] M.L. Andersen, L.H. Skibsted, Electron Spin Resonance Spin Trapping Identification of Radicals Formed during Aerobic Forced Aging of Beer Mogens, J. Agric. Food Chem. 8561 (1998) 1272–1275.

[71] R.J. Elias, M.L. Andersen, L.H. Skibsted, A.L. Waterhouse, Identification of free radical intermediates in oxidized wine using electron paramagnetic resonance spin trapping, J. Agric. Food Chem. 57 (2009) 4359–4365. doi:10.1021/jf8035484.

[72] E.C. Pascual, B.A. Goodman, C. Yeretzian, Characterization of free radicals in soluble coffee by electron paramagnetic resonance spectroscopy, J. Agric. Food Chem. 50 (2002) 6114–6122. doi:10.1021/jf020352k.

[73] S. Xia, C. Tan, Y. Zhang, S. Abbas, B. Feng, X. Zhang, F. Qin, Modulating effect of lipid bilayer-carotenoid interactions on the property of liposome encapsulation, Colloids Surfaces B Biointerfaces. 128 (2015) 172–180. doi:10.1016/j.colsurfb.2015.02.004.

[74] B. Tonyali, A. McDaniel, V. Trinetta, U. Yucel, Evaluation of heating effects on the morphology and membrane structure of Escherichia coli using electron paramagnetic

resonance spectroscopy, Biophys. Chem. 252 (2019) 101191. doi:10.1016/j.bpc.2019.106191.

[75] A. Pegi, K. Julijana, P. Slavko, Š. Janez, Š. Marjeta, The Effect of Lipophilicity of Spin-Labeled Compounds on Their Distribution in Solid Lipid Nanoparticle Dispersions Studied by Electron Paramagnetic Resonance, J. Pharm. Sci. 92 (2003) 58–66. doi:10.1002/jps.10277.

[76] U. Yucel, R.J. Elias, J.N. Coupland, Localization and reactivity of a hydrophobic solute in lecithin and caseinate stabilized solid lipid nanoparticles and nanoemulsions, J. Colloid Interface Sci. 394 (2013) 20–25. doi:10.1016/J.JCIS.2012.12.042.

[77] C.C. Berton-Carabin, J.N. Coupland, R.J. Elias, Effect of the lipophilicity of model ingredients on their location and reactivity in emulsions and solid lipid nanoparticles, Colloids Surfaces A Physicochem. Eng. Asp. 431 (2013) 9–17. doi:10.1016/j.colsurfa.2013.04.016.

[78] P. Ahlin, J. Kristl, M. Šentjurc, J. Štrancar, S. Pečar, Influence of spin probe structure on its distribution in SLN dispersions, Int. J. Pharm. 196 (2000) 241–244. doi:10.1016/S0378-5173(99)00431-7.

Chapter 3 - Objectives

The goal of this research was to develop a further understanding of delivery systems for small molecules that can be used in food, cosmetic, and drug industries. Because many of these functional or bioactive ingredients have poor stability, they require a delivery system for protection. Further, there is a growing interest in the field of controlled release encapsulated ingredients, with controlled destabilization of the delivery system (such as a change in environmental pH). There is a need to further understand how hydrophobic ingredients behave *in-situ* when loaded into a delivery system. To do this, electron paramagnetic resonance spectroscopy (EPR) can be used to study a model hydrophobic ingredient, or spin probe, within a delivery system. Although this technique requires the use of a model ingredient, it can provide information as to the location of the model ingredient without destroying the delivery system.

The first objective of this study was to formulate a pH-sensitive colloidosome structures composed of food-grade ingredients, using palmitic acid in caseinate-stabilized solid lipid nanoparticles (SLN) as the shell particles and a refined coconut oil lecithin-stabilized liquid lipid nanoparticle (LLN) reservoir as a center particle. I hypothesized that colloidosome structures can be formed by electrostatic deposition of positively charged SLN onto the LLN surface, which can serve as a pH-triggered release mechanism by controlling the migration of ingredients out of LLN. The formation of colloidosomes will be evaluated by mixing SLN and liquid lipid particles at different mixing ratios, i.e. increasing the ratio of SLN in the mixture, to investigate the ratio where colloidosomes are sufficiently covered to avoid bridging flocculation. The formulated ratio of SLN and LLN colloidosomes will then be loaded with a model hydrophobic, ingredient the electron paramagnetic resonance (EPR) active spin probe 4-phenyl-2,2,5,5-tetramethyl-3-imidazoline-1-oxyl nitroxide (PTMIO), to study the distribution of the ingredient during an

ascorbate assay to understand how hydrophobic ingredients are released from the colloidosome structures. Because ascorbate is largely hydrophilic, it is expected to only deplete the PTMIO in the aqueous phase. As the ascorbate reaction progresses, PTMIO from an emulsion's surface has previously been shown to migrate into the continuous phase (out of the emulsion). With the addition of a solid barrier at pH 3.5, by the electrostatic deposition of SLN to the liquid nanoparticle surface, the first order reaction rate constant of the ascorbate reaction will be lesser at pH 3.5 than at pH 7. To analyze differences in particle size, zeta potential, and the transport kinetics of PTMIO, data was collected in a completely randomized design and analyzed as a two by two factorial where pH (either 3.5 or 7) and either the addition of SLN or water are analyzed.

The second objective is to create liposomal vesicles (LV) with saturated (80H and 90H) and unsaturated (PC75 and 90G) lecithins. I hypothesized the model hydrophobic ingredient (PTMIO) loaded into nanovesicles formed with saturated lecithins will have lesser reactivity with an aqueous reactant because the vesicles have a more rigid structure. Because LV can assume various morphologies, they will be loaded with refined coconut oil to act as a guest molecule to understand how the fatty acid tails incorporate foreign chemicals. With the addition of a guest molecule, space within LV will be limited. Therefore, the packing of the LV with different lecithins will be studied by differential scanning calorimetry (DSC). DSC will provide insights to the physical state of the membrane, i.e., crystallization of the fatty acid tails of LV will be greater in lecithins with saturated fatty acid tails. Lastly, LV will be loaded prepared with PTMIO and undergo an ascorbate assay to track the distribution of PTMIO *in-situ*, deconvolute EPR spectra to understand how PTMIO associate in LV with saturated and unsaturated fatty acid tails. Simulation show the location of the spin probes within the LV. If lecithins with unsaturations make more permeable LV, then the reaction rate of PTIMO reduction by ascorbate

will be lesser for LV made with saturated lecithins. Data was collected in a completely randomized design, the effects of lecithin (PC75, 90G, 90H, or 80H) and carrier lipid fraction (0%, 0.5%, or 1.0%) were analyzed in a factorial.

Chapter 4 - Nano-structured lipid particles for controlled transport of hydrophobic volatile and nonvolatile molecules

4.1. Abstract

Nano-structured particles can be designed for tailored delivery of small molecules. The self-assembled nano-emulsion structures (i.e., colloidosomes) were formed via electrostatic deposition of solid wall around a liquid reservoir. Liquid lipid nanoparticles (LLN) stabilized by lecithin and solid lipid nanoparticles (SLN) stabilized by sodium caseinate were used as food-grade systems. The particle size and zeta potential measurements were used at pH 3.5 and 7 to characterize the colloidal dispersions at selected mixing ratios (2:1 to 1:5). The partitioning, kinetic release, and reactivity of non-volatile (4-phenyl-2,2,5,5-tetramethyl-3-imidazoline-1-oxyl nitroxide; PTMIO) and volatile (limonene) molecules were studied using electron paramagnetic resonance (EPR) spectroscopy and atmospheric pressure chemical ionization-mass spectroscopy (APcI-MS), respectively, as a function of pH-change at the optimal 1:3 ratio. Particle size of LLN (134 nm) and SLN (166 nm) remained unchanged with pH adjustment, and colloidosome particle size (450 nm) was combination of LLN and SLN particles at pH 3.5. The presence of the solid wall significantly reduced the diffusion rate (ca. 80%) of PTMIO from the reservoir protecting the compound in LLN core. APcI-MS measurements showed similar behavior for limonene release to air. These systems can be used for controlled delivery of various active compounds in food and pharmaceutical formulations.

4.2. Introduction

Emulsions are abundant in a variety of food products as well as in cosmetic and pharmaceutical formulations. Emulsions can bind small molecules changing their phase behavior, stability, reactivity, as well as bioavailability [1]. In addition, versatility of emulsions allows for them to be structured for effective and efficient delivery of labile and hydrophobic small molecules, such as antimicrobials, antioxidants, poly-unsaturated oils, vitamins, flavors, etc. [2–8].

Earlier approaches considered manufacturing emulsions with nano-scale lipid droplets, known as nano-emulsions (i.e., particles smaller than 200 nm where the interfacial region does not account more than 10% of total volume) for improved physical stability of the dispersed phase and increased bioavailability of the active ingredients [9]. However, these benefits are negated by inefficient control of the release kinetics and increased reactivity of the encapsulates associated with very short diffusion pathways and large interfacial areas [3, 4, 9]. Subsequently, researchers attempted to control the release kinetics of encapsulated ingredients by encapsulating them in a solid lipid matrix, often referred as solid lipid nanoparticles, with an idea of forming a homogenously distributed solid dispersion [11].

Crystallization of nano-scale lipid particles, however, resulted in exclusion of the hydrophobic ingredient from the incompatible solid lipid matrix, known as burst release [3]. The rapid polymorphic transitions to the higher density crystal structures at nano-scale dimensions was the main reason of this phenomenon [11]. The following approach has been to structure the nanoparticles by forming a solid shell around a liquid core, which serves as a reservoir for the lipophilic ingredient. The main challenge has been the formation of solid wall surrounding the liquid core and keeping the wall stable. Some attempts included surface heterogenous

crystallization using high-melting phospholipids [12]. The polymorphic transitions and lipid migration can still be a concern for their storage stability [13].

Another way of forming a solid barrier is by the adsorption of solid particles around a liquid droplet as seen in Pickering emulsions. Pickering-stabilized systems are associated with high absorption energies, which can limit the control over the solid wall structure [7]. Alternatively, similar structures can be formed by electrostatic assembly of solid particles around a liquid reservoir. The name colloidosome was first introduced in 2002, for systems where a liquid lipid core is covered by solid polystyrene particles [14]. Later, Gu and McClements showed that similar systems can be formed by the deposition of oppositely charged emulsion droplets as a function of droplet size relative to the fractions of individual emulsion phases [15].

There is a need to understand the real-time behavior of encapsulated ingredients including their localization, release kinetics, and reactivity for applications in controlled release of hydrophobic ingredients to produce systems that can be used for triggered release of small molecules. Electron paramagnetic resonance (EPR) spectroscopy is a technique based on the interaction of molecules bearing unpaired electrons with an external magnetic field. Historically, EPR spectroscopy has been used to study free radical reactions both *in vivo* and *in vitro* [16]. Alternatively, an EPR spin-labeling technique (e.g., using stable nitroxide spin probes) can be used for structural characterization of colloidal dispersions, such as solid lipid nanoparticle distribution and transport kinetics of encapsulated small molecules [4,13,17,18].

The real-time release kinetics of small volatile molecules from complex food dispersions can be characterized by using an atmospheric pressure chemical ionization-mass spectroscopy (APcI-MS) technique [19,20]. This technique samples volatiles from sample headspace, or even

from oral cavity of humans, to provide direct information about active flavor compound concentrations leading to aroma perception.

The objectives of this chapter are to produce self-assembled colloidal aggregates to encapsulate volatile (limonene) and non-volatile hydrophobic (a model hydrophobic spin probe) small molecules via interfacial electrostatic interactions, which are sensitive to pH change. Their phase behavior, release kinetics, and reactivity were characterized using EPR spectroscopy and APcI-MS techniques.

4.3. Materials and methods

4.3.1. Materials

Sodium ascorbate, ferric chloride, and sodium caseinate were purchased from Alfa Aesar (Ward Hill, MA); 4-phenyl-2,2,5,5-tetramethyl-3-imidazoline-1-oxyl nitroxide (PTMIO, >95% purity) was purchased from Enzo Life Sciences (Plymouth Meeting, MI); glacial acetic acid and sodium acetate were purchased from Fisher Scientific (Lenexa, KS). All chemicals were analytical grade and used without further modification. Phosphatidylcholine-75 (PC75) containing saturated myristic acid (75%) was purchased from Lipoid LLC (Newark, NJ). Hydrogenated palm stearin, with a melting point between 55-58°C, was donated by Cargill (Minneapolis, MN, USA). Refined coconut oil composed of 1:1 caprylic and capric acids (i.e., as determined by methyl ester analysis using GC-MS), with a melting point below 0°C, was purchased from a local supermarket.

4.3.2. Emulsion Preparation

Solid lipid nanoparticles (SLN) and liquid lipid nanodroplets (LLN) were prepared from sodium caseinate (4 wt%) plus hydrogenated palm stearin (40 wt%) and PC75 (3.4 wt%) plus

refined coconut oil (10 wt%), respectively. In brief, firstly the encapsulates non-volatile PTMIO (to a final concertation of 200 μM in the emulsion) or volatile limonene (to a final concentration of 100 ppm in the emulsion) was added to the refined coconut oil as a carrier lipid. The lipid phase then mixed with the aqueous phase solution (mixed on a magnetic stir plate while heated to ca. 60°C for 1 h) using a high shear mixer (Ultra Torrax, Ika Works, Wilmington, NC) at 24,000 rpm for 1 min to obtain coarse emulsions. The coarse emulsion was further homogenized using a 2-stage valve homogenizer (Panda Plus 2000, GEA Niro Soavi, Parma, Italy) at 500 bar (where the second stage is set to 50 bar and the total pressure is set to 500 bar with the first stage), at ca. 65°C, for 3 passes. Emulsions were stored at refrigerated conditions overnight to allow complete crystallization of SLN.

4.3.3. Formation of Self-assembled Particles

Self-assembled aggregates of LLN and SLN emulsions, also referred as colloidosomes, were prepared by a using a similar method described by Gu, Decker, & McClements [15]. The pH values of the final emulsions were adjusted to 3.5 and 7 by adding aliquots of 1 M HCl or NaOH with agitation. LLN and SLN emulsions were mixed by slow (5 mL/min) addition of LLN to SLN at ratios of 2:1, 1:1, 1:2, 1:3, 1:4, and 1:5. The oppositely charged LLN and SLN electrostatically attract each other at pH 3.5 to form a SLN coating on LLN. The same mixtures with the same electrostatic charge at pH 7 serve as negative controls.

4.3.4. Particle Size and Zeta Potential Determination

The emulsions and colloidal mixtures were characterized for their particle size (d_{32}) and zeta potential using DelsaMax Pro (Beckman Coulter, Brea, CA) with a flow cell attachment and DelsaMax Assist unit. Diameter values are reported as the Sauter mean diameter (d_{32}).

Emulsions were diluted (1:200 v/v in acetate buffer (50 mM) at the respective pH to avoid multiple scattering effects.

4.3.5. EPR Spectroscopy Measurements

EPR spectroscopy was used to analyze the distribution and transport kinetics (i.e., related to longitudinal diffusivity) of the hydrophobic ingredient, PTMIO, as a function of colloidal structure. Briefly, 10 mL of LLN, SLN, or their mixtures was degassed with humidified (i.e., to prevent evaporation) nitrogen gas (ca. 3 L/min) for 15 min. Aliquots of samples (50 mL) were then transferred into borosilicate capillary tubes under nitrogen and sealed with vinyl plastic putty (Leica Microsystems, Wetzlar, Germany). The samples were analyzed at room temperature in an EPR spectrometer (SpinscanX, ADANI, Minsk, Belarus) operating at X-band. The samples were analyzed under the following measurement conditions: center field 335.5 mT, sweep width 6.0 mT, modulation frequency 100 kHz, modulation amplitude 100 uT, microwave power 6.3 mW. EPR spectra were simulated using the WinSim2002 software (version 0.98, National Institute of Environmental Health Sciences, NIH, Bethesda, MD) for deconvoluting EPR signals of PTMIO in environments with distinct polarities [2,3].

The reactivity and transport properties of the spin probe was determined using a protocol described by Yucel et al. [1, 2]. Sodium ascorbate (2 mM) and ferric chloride (10 μM) were added to samples (10 mL) under deoxygenated conditions to reduce PTMIO to its EPR-silent form. Within 30 seconds of the addition of the reagents, aliquots of the mixture (50 μL) were collected in sealed borosilicate capillary tubes. EPR spectra were collected at 2-minute intervals over 30 minutes. The fraction of EPR-active PTMIO in the aqueous and lipid fractions were calculated as a function of time to assess the diffusion effects on the probe reactivity. Following

the reaction progress, release kinetics were quantified using apparent first order kinetics and linear regression.

4.3.6. Statistical Analysis

All experiments were performed in triplicate. The effects of formulations on the particle size and zeta potential of emulsion and emulsion aggregates, and the release kinetics of the encapsulates from colloidal aggregates were analyzed by analysis of variance (ANOVA) using a general linear model. Post-ANOVA Tukey`s multiple comparison test was applied to evaluate the differences between treatments. Significance was considered at ($p < 0.05$). Statistical analysis was performed in Minitab v17 (State College, PA).

4.4. Results and discussion

4.4.1. Physical Properties of LLN and SLN Emulsions

To find homogenization conditions that for subsequent analysis, 10% tetradecane with either 4% sodium caseinate or 3.4% Phospholipon PC75 (a trade name for phosphatidylcholine) emulsions were made high-pressure homogenization at 100 bar, 500 bar, or 1000 bar. Emulsions were stored at 4°C and measured for their particle size daily for five days (Figure A.1). Emulsions made at 100 bar had both greater particle sizes for both caseinate and PC75 emulsions. Although caseinate emulsions made at 1000 bar are ca. 20 nm diameter smaller than 500 bar, PC75 emulsions are similar at the two pressures. Although using 1000 bar pressure further decreases the particle size, emulsions made at 500 bar pressure have similar particle sizes. The selected homogenization pressure was 500 bar because it had lesser error and produced smaller particles than the 100-bar emulsions.

The pH of LLN and SLN emulsions were adjusted of 3.5 and 7 immediately after their preparation before crystallization of SLN. The pH adjustment didn't affect ($p > 0.05$) the particle size distribution of both emulsions, which were unimodal and narrow (PDI 10 ± 1) with Sauter mean diameters (d_{32}) of 166 ± 10 nm and 135 ± 10 nm for SLN and LLN, respectively (Figure 4.1). The small but significantly ($p < 0.05$) larger particle size of SLN particles are mainly due to the crystallization phenomenon, which slightly distorted the spherical shape at nanoscale dimensions [2]. In addition, the lecithin is also responsible for formation of slightly smaller particles at the nanoscale, however the particle size of SLN and LLN were similar ($p > 0.05$) prior to crystallization, in agreement with previous findings [3].

LLN and SLN were both negatively charged at pH 7 (Figure 4.1c). When SLN emulsions prepared with sodium caseinate was adjusted to pH 3.5 below the isoelectric point of the protein, the surface charge potential became positive. LLN emulsions prepared with lecithin retained their negative charge at pH 3.5 (Figure 4.1c). Therefore, combining oppositely charged particles at controlled conditions can result in formation of self-assembled structures, such as colloidosomes [15].

The combination of the two emulsion systems needs to be done with care in order to prevent bridging flocculation and undesirable gelation. The first step was to investigate the effect of mixing ratio of LLN and SLN for the formation of stable colloidosomes. The particle size and zeta potential of LLN and SLN mixtures were measured in combination with their physical appearance (i.e., gelation) at different ratios (2:1, 1:1, 1:2, 1:3, 1:4, and 1:5 LLN:SLN). Up to mixing ratio of 1:2 the mixtures gelled with multimodal PDI (Figure 4.3). This suggests that uncovered LLN interacts with SLN on the surface of the other LLN resulting in bridging flocculation. This is visually depicted in Figure 4.4. These bridges are expected when the

fraction of LLN is high because insufficient SLN is present to cover the entire surface. Bridging flocculation has been observed in mixtures of oppositely charged systems [22].

At higher ratios (1:3 and above) the particle size of the colloidosome aggregates equilibrated at 400 nm in diameter (Figure 4.3a). However, the formation of the colloidosome structure needs to be done with care to prevent bridging flocculation. LLN emulsions were slowly (5 mL/min) added to SLN emulsions on a magnetic stirrer and allow to mix completely. At higher ratios, the polydispersity index increases as particle size of excess SLN converges the average particle size to 200 nm (Figure 4.3b). Indeed, the mixture has bimodal particle size distribution with a lesser peak at 160 nm, and a larger peak at 530 nm (Figure 4.2a). In other words, the intensity of the split peak observed for non-associated SLN particles at 160 nm in Figure 4.2 increases gradually. Similar to our observations, Gu et al. investigated the addition of cationic small particles to anionic large particles, finding that the overall particle size decreases as the concentration of small droplets increases [15]. This is because as more unadsorbed SLN particles are in the solution, the average particle size observed is a lesser value. The same LLN:SLN mixture at pH 7, however, was not significantly different from the individual components ($p > 0.05$; Figure 4.1a). At pH 7, because both LLN and SLN are negatively charged, it is expected that no self-assembly occurred. While various mixtures were examined for the formation of colloidosomes, the LLN:SLN ratio of 1:3 was selected for further experiments and is the only mixture referred herein. This ratio was chosen because sufficient exterior particles are present to cover the LLN surface, while not having superfluous exterior particles. The colloidosome particles (LLN:SLN mixtures of 1:3 at pH 3.5) had a particle size (d_{32}) of 450 ± 10 nm in diameter and a zeta potential of 32.48 ± 2.01 mV (Figure 4.1).

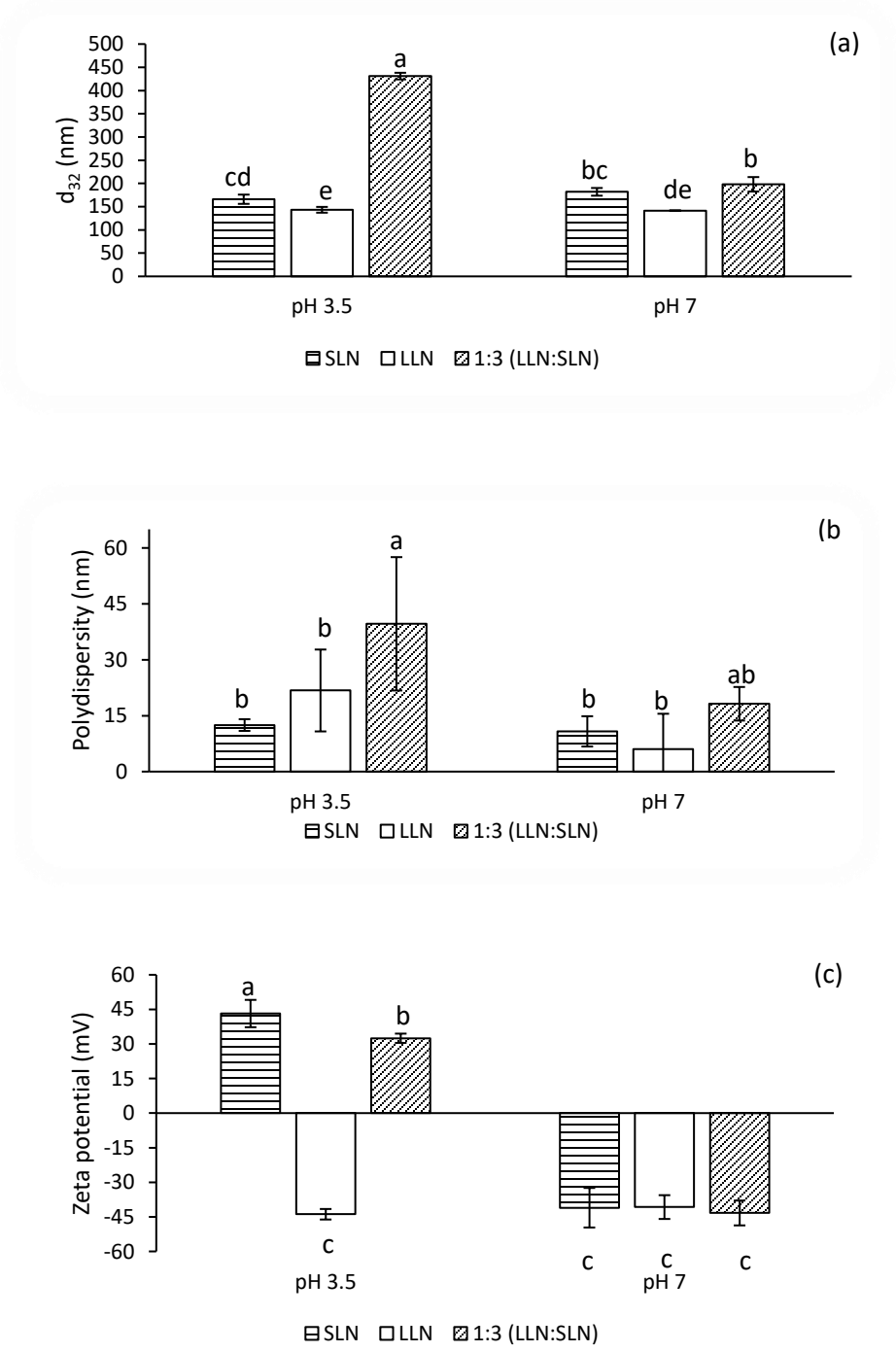

Figure 4.1. d32 (a), polydispersity (b), and zeta potential (c) of LLN, S LN, and their mixture (1:3) at pH 3.5 and pH 7. Results that do not share letters are significantly different.

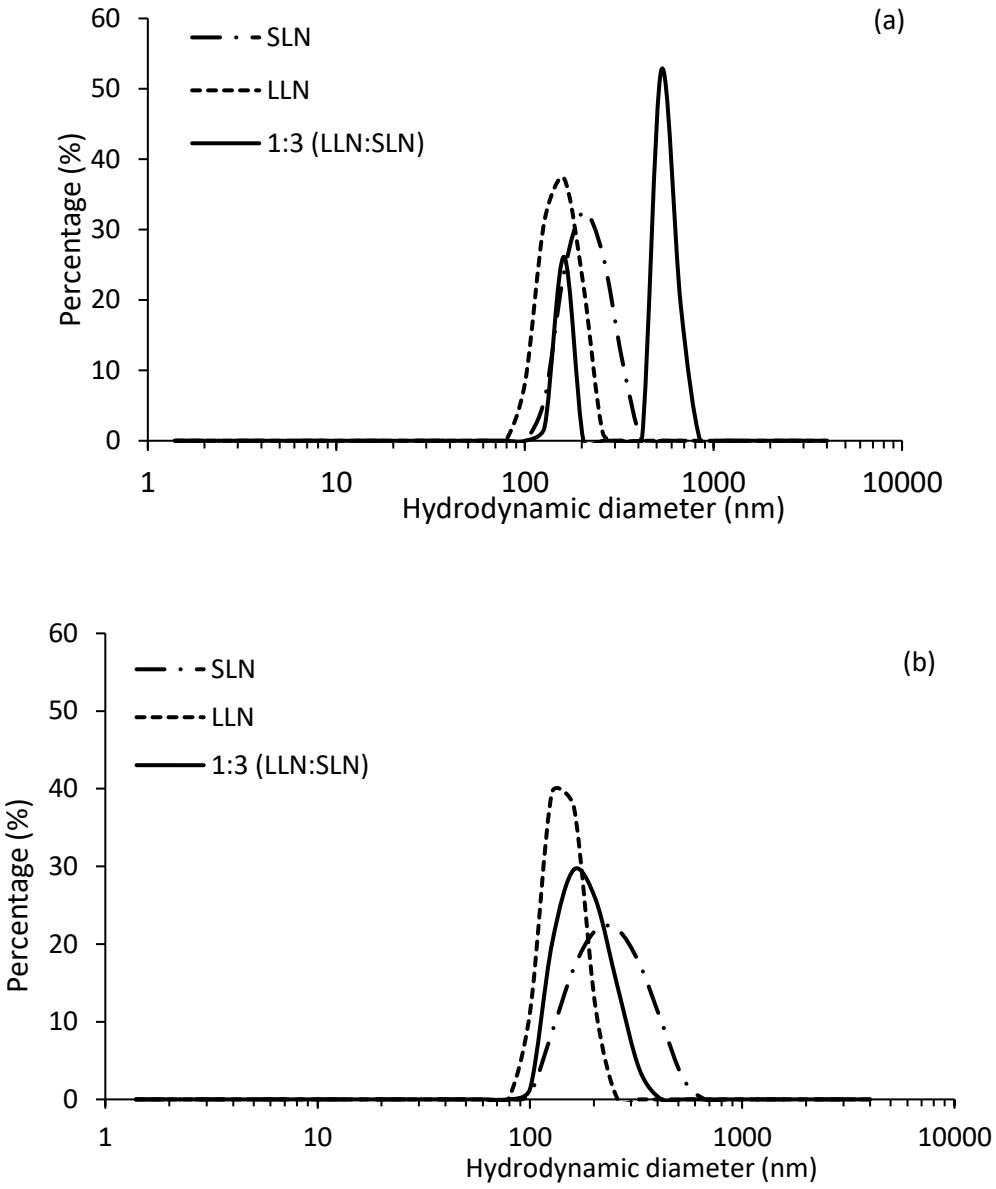

Figure 4.2. Particle size distribution of LLN, SLN, and their 1:3 mixture at pH 3.5 (a) and pH 7 (b).

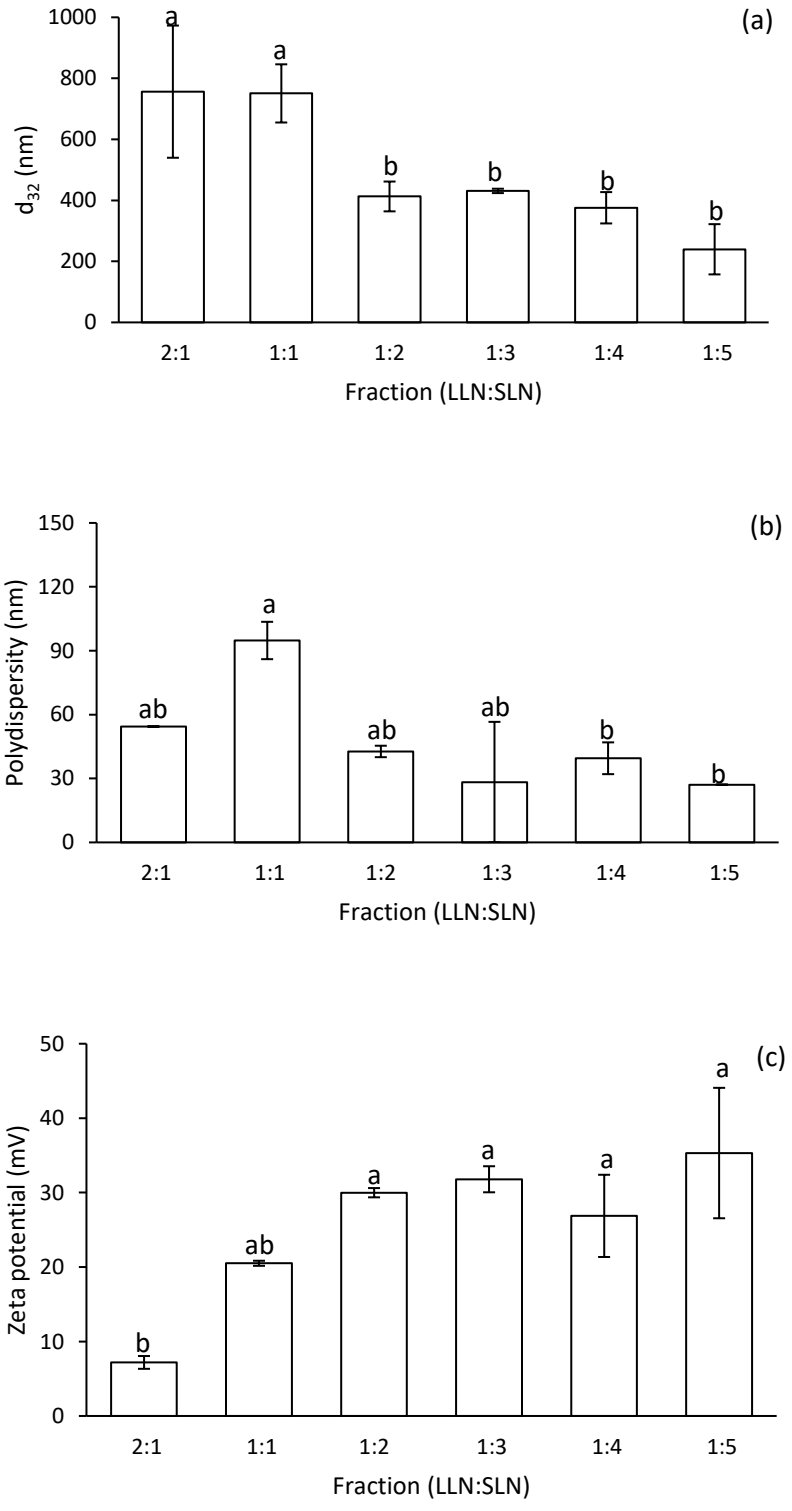

Figure 4.3. d_{32} (a) and zeta potential (b) of mixtures of LLN and SLN at different mixing ratios. Results that do not share letters are significantly different.

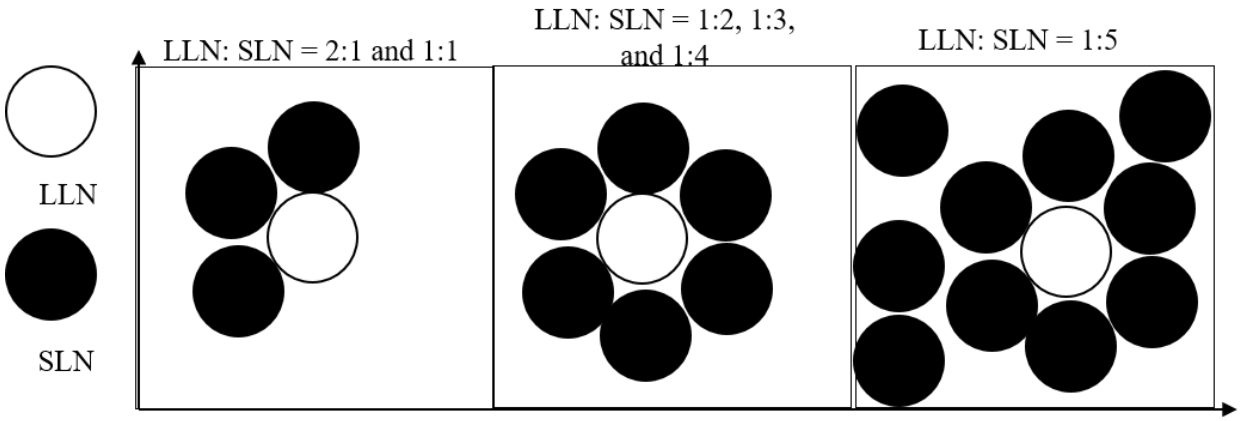

Figure 4.4. Schematic drawing of colloidosome structures formed at different ratios of LLN:SLN.

4.4.2. Analysis of PTMIO distribution and diffusion

EPR spectroscopy was used to understand the distribution and behavior of hydrophobic ingredients in the designed nano-structured colloidal systems. PTMIO was selected as a model molecule for its hydrophobic characteristics, having a *log P* value of 2.5, and was expected to behave similarly to hydrophobic ingredients in food and drug formulations.

EPR spectra of PTMIO in an emulsion showed the characteristic nitroxide triplet with distinct hyperfine splitting constants (a_N) for aqueous and lipid fractions (Figure 4.5). To resolve EPR spectra of PTMIO in dispersions, spectra were simulated using the technique described in our previous studies [2-4]. This technique runs a downhill simplex to resolve complex EPR spectra and deconvolute PMTIO in chemically unique environments. The lipid fraction signal was distinct by a_N of 1.66 mT from the aqueous fraction a_N of 1.65 mT in LLN. Majority ($2/3^{rd}$) of the PTMIO partitioned into the lipid phase, and the rest (ca. $1/3^{rd}$) in the aqueous phase, where

it is biochemically reactive. The change in the pH didn't significantly ($p < 0.05$) affect the lipid-aqueous phase equilibrium. The lipid signal was previously shown to be lost in SLN emulsions due to expulsions of the encapsulate from the droplet core with crystallization [2-4]. In the present study, SLN did not contain the hydrophobic molecule but used as solid wall-forming particles.

The EPR spectra from colloidosome structures formed at pH 3.5 were similar to that from LLN (Figure 4.5), however with a difference in the high-field peak shape. In order quantify the amount of change, the EPR spectra was simulated, and the complex spectra was deconvoluted to individual contributions coming from aqueous and lipid phases (Figures 4.5 and 4.7). The aqueous PTMIO in LLN was slightly (ca. 10%) but significantly ($p < 0.05$) larger than that in colloidosome systems. This is due to presence of more lipid particles and larger surface area in the colloidosome systems. Regardless, the a_N for lipid and aqueous fractions remain unchanged in water-diluted LLN and colloidosome samples indicating the simulation process is capable of effectively separating individual contribution of the PTMIO from respective phases. While the EPR spectra are insightful to determine the distribution of hydrophobic ingredients in dispersion, the main effect of forming a solid wall around a liquid reservoir is to control the transport properties of the encapsulated molecule. For this reason, we analyzed the reduction of PTMIO to an EPR-silent form in LLN emulsions and the 1:3 mixtures of LLN and SLN at pH 3.5 and 7. The concertation of EPR-active PTMIO was monitored for a reaction period of 30 minutes following the addition of ascorbate (Figure 4.6). The signal intensities were calculated by double-integration of the EPR spectra at each discrete time points.

In LLN emulsions PTMIO was reduced quickly both at pH 3.5 and 7 (Figure 4.6) with a similar first order reaction rate constants (k values) (Table 1). In nano-emulsions, Yucel et al.

previously showed that ascorbate reduction of PTMIO is not a diffusion-limited process [2]. In other words, the diffusion rate is significantly greater than that of the reduction reaction that takes place in the aqueous phase. When the aqueous fraction was replaced with SLN to form colloidosomes at a ratio of 1:3 (LLN:SLN), the k values significantly decreased at both pH values (Table 1). Although colloidosome structured was not formed in LLN:SLN mixture at pH, the reaction rate was 35% smaller than LLN samples at the same pH. This is probably related to the depletion effects from excess SLN particles. By the end of the reaction period of 30 min, more than 80% of the PTMIO was reduced. When a solid wall formed around the LLN as PTMIO reservoir at pH 3.5, the reaction rate was decreased 80%. Indeed, by the end of the reaction period of 30 min, 65% of the PTMIO was still remain protected in the LLN reservoir. Moreover, SLN and the related colloidosomes assume a positive charge at pH 3.5 (Figure 4.1). The anionic ascorbate ions were expected to have high affinity for cationic colloidosome surfaces, and to localize there increasing the rate of the reduction reaction and quench PTMIO [23]. Our results, therefore, indicate that the reaction rate was diffusion-limited in the presence of solid wall. As a further evidence, the fraction of PTMIO in lipid and aqueous phases were simultaneously calculated throughout the reaction period from the deconvoluted EPR spectra (Figure 4.7).

Similar to previous findings [3], the a_N for the lipid and aqueous contributions remained unchanged throughout the reaction period indicating our measurements and simulations represented the actual phase distribution of the PTMIO. In colloidosome emulsions (pH 3.5) the PTMIO in the lipid phase gradually increased from 71% to 85% (i.e., along with a decrease of the aqueous fraction from 2 9% to 15%) (Figure 4.7a). The phase-partitioning of PTMIO in SLN:LLN mixtures at pH 7, however, remained unchanged throughout the reaction period

indicating that the diffusion path of PTMIO across the LLN so small to show any significant effect (Figure 4.7b). In colloidosome particles, although the length of the diffusion path is comparable to that in LLN, the migration of PTMIO to the aqueous phase, where it can react, was limited with a tortuous solid wall.

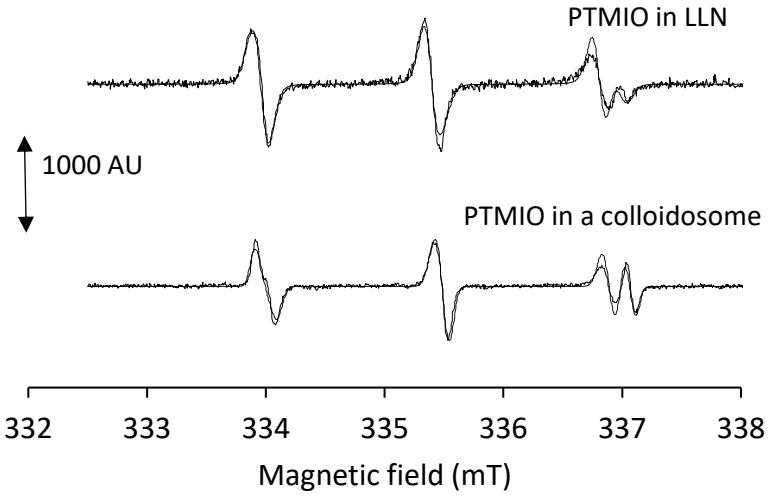

Figure 4.5. Typical EPR spectra and simulation of PTMIO in a LLN and colloidsome.

4.4.3. Real-Time APcI-MS Measurement of Limonene Release

The real-time release kinetics of limonene from emulsions and colloidosome aggregates to the air was studied by using real-time APcI-MS. After aliquots of samples are equilibrated at 30 °C in a deactivated and sealed glass vessel for at least 30 min, the headspace air was sampled at 200 mL/min and continuously monitored for limonene concentration with MS coupled to APcI probe. In order to prevent vacuum in the glass vessel, humidified high-purity air was introduced through a separate port. The flow rate was monitored continuously throughout the MS measurements with a deviation of 15 mL/min. The limonene release from LLN to the surrounding air was constant for the first 10 minutes followed by a gradual decrease (Figure. A.3). The pH change didn't show a significant effect to the limonene release from LLN.

However, in colloidosome particles, where LLN as limonene reservoir surrounded by SLN, the diffusion was limited as compared to LLN observed as a faster decrease in headspace limonene (Figure A.3). This indicates a diffusion-limited release mechanism similar to that observed for EPR experiments. After 40 min, the pH was adjusted to neutral by adding aliquots of NaOH through one of the injection ports on the glass reaction vessel. After pH adjustment and re-equilibration of 5 min (waiting time was not shown on the graph), the limonene was regenerated at the headspace. The blue line in Figure A.3 shows the control for LLN:SLN (1:3) mixture emulsions at pH 7, where no pH adjustment was done. The resulting amount of limonene in the headspace of colloidosome was double the amount of LLN samples after breaking of the colloidosome structure.

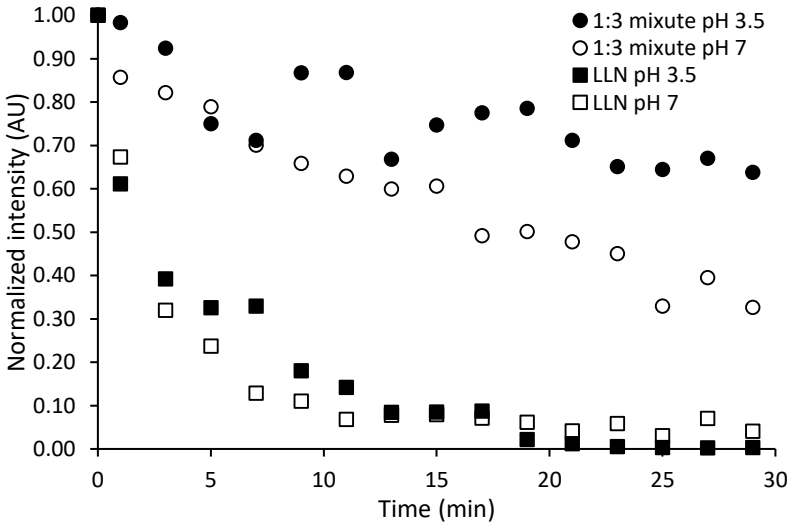

Figure 4.6. Typical reaction kinetics of ascorbate-PTMIO reaction in LLN and the 1:3 (LLN:SLN) mixture at pH 3.5 and 7.

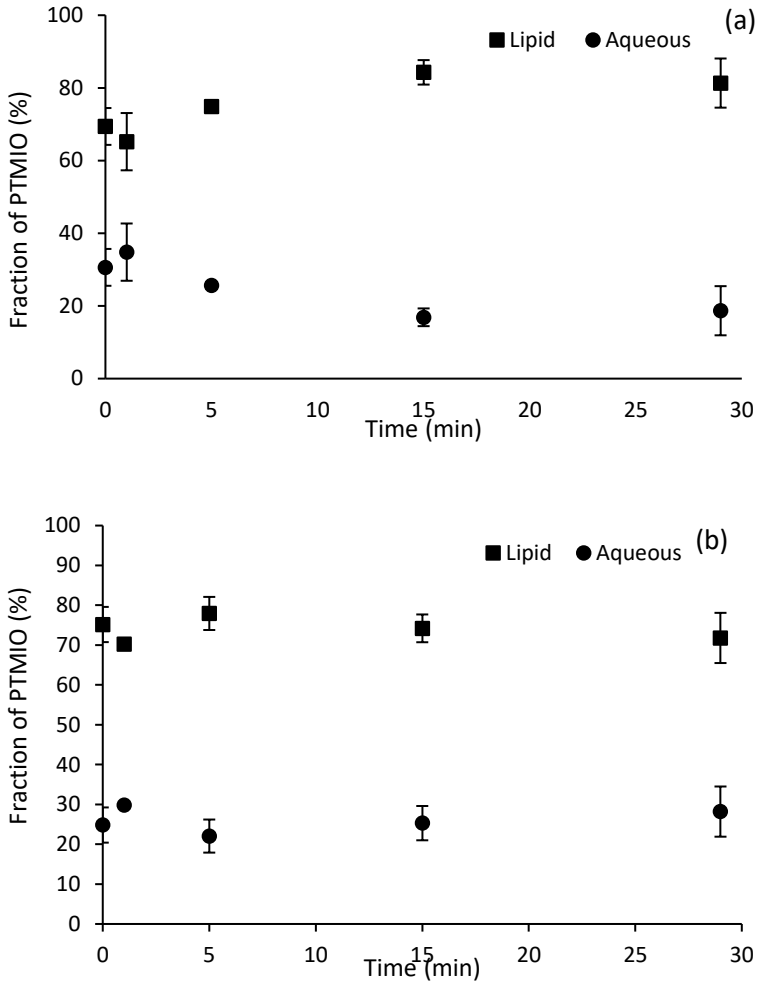

Figure 4.7. Fractions of PTMIO in lipid and aqueous environments in colloidosome mixtures at pH 3.5 (a) and pH 7 (b).

Table 4.1. First-order reaction rate constant, k (min^{-1}), of PTMIO reduction by ascorbate at pH 3.5 and pH 7.

Sample	k (min^{-1}) at pH 3.5	k (min^{-1}) at pH 7
LLN dilution in water	$1.71 \times 10^{-1} \pm 3.43 \times 10^{-2}$	$8.36 \times 10^{-2} \pm 1.29 \times 10^{-2}$
LLN mixture with SLN	$2.91 \times 10^{-2} \pm 1.43 \times 10^{-2}$	$5.78 \times 10^{-2} \pm 2.08 \times 10^{-2}$

4.5. Conclusion

In this study, we showed that colloidal aggregates can be developed in the form of colloidosome structures by electrostatic deposition of oppositely charged nanoparticles. This allows coating a liquid reservoir with solid particles to create a barrier for limiting the diffusion of encapsulated ingredients. The integrity of the solid barrier can be controlled as a function of pH. EPR and real-time APcI-MS measurements were used to evaluate the transport properties of volatile and nonvolatile small hydrophobic molecules from designed colloidal systems. The formation of solid shell does not affect the distribution of encapsulated ingredients but controls the diffusion rates affecting their reactivity and bioavailability. These systems can provide great potential for guided and controlled delivery of hydrophobic functional molecules, such as flavors, phytochemicals, antioxidants, etc. in functional food and pharmaceutical applications.

4.6. References

[1] D.J. McClements, Edible nanoemulsions: Fabrication, properties, and functional performance, Soft Matter. 7 (2011) 2297–2316. doi:10.1039/c0sm00549e.

[2] U. Yucel, R.J. Elias, J.N. Coupland, Solute distribution and stability in emulsion-based delivery systems: An EPR study, J. Colloid Interface Sci. 377 (2012) 105–113. doi:10.1016/J.JCIS.2012.03.071.

[3] U. Yucel, R.J. Elias, J.N. Coupland, Localization and reactivity of a hydrophobic solute in lecithin and caseinate stabilized solid lipid nanoparticles and nanoemulsions, J. Colloid Interface Sci. 394 (2013) 20–25. doi:10.1016/J.JCIS.2012.12.042.

[4] U. Yucel, R.J. Elias, J.N. Coupland, Effect of liquid oil on the distribution and reactivity of a hydrophobic solute in solid lipid nanoparticles, J. Am. Oil Chem. Soc. 90 (2013) 819–824. doi:10.1007/s11746-013-2228-x.

[5] V. Trinetta, M.T. Morgan, J.N. Coupland, U. Yucel, Essential oils against pathogen and spoilage microorganisms of fruit juices: use of versatile antimicrobial delivery systems, J. Food Sci. 82 (2017) 471–476. doi:10.1111/1750-3841.13614.

[6] J. Ghosh, S; Peterson, DG; Coupland, Effects of droplet crystallization and melting on the aroma release properties of a model oil-in-water emulsion, J. Agric. Food Chem. 54 (2006) 1829–1837. doi.org/10.1021/jf052262w (accessed October 5, 2018).

[7] R. V. Tikekar, Y. Pan, N. Nitin, Fate of curcumin encapsulated in silica nanoparticle stabilized Pickering emulsion during storage and simulated digestion, Food Res. Int. 51 (2013) 370–377. doi:10.1016/J.FOODRES.2012.12.027.

[8] H.M.C. Azeredo, K.W. Waldron, Crosslinking in polysaccharide and protein films and coatings for food contact - A review, Trends Food Sci. Technol. 52 (2016) 109–122. doi:10.1016/j.tifs.2016.04.008.

[9] E. Acosta, Bioavailability of nanoparticles in nutrient and nutraceutical delivery, Curr. Opin. Colloid Interface Sci. 14 (2009) 3–15. doi:10.1016/j.cocis.2008.01.002.

[10] Q. Wang, T. Gong, X. Sun, Z. Zhang, Structural characterization of novel phospholipid lipid nanoparticles for controlled drug delivery, Colloids Surfaces B Biointerfaces. 84 (2011) 406–412. doi:10.1016/j.colsurfb.2011.01.034.

[11] S. Müller, RH, Mäder, K, Gohla, Solid lipid nanoparticles (SLN) for controlled drug

delivery - a review of the state of the art, Eur. J. Pharm. Biopharm. 50 (2000) 161–170. doi:10.1016/s0928-0987(97)86243-4.

[12] H. Salminen, T. Helgason, B. Kristinsson, K. Kristbergsson, J. Weiss, Formation of solid shell nanoparticles with liquid ω-3 fatty acid core, Food Chem. 141 (2013) 2934–2943. doi:10.1016/j.foodchem.2013.05.120.

[13] M. Samtlebe, U. Yucel, J. Weiss, J.N. Coupland, Stability of solid lipid nanoparticles in the presence of liquid oil emulsions, JAOCS, J. Am. Oil Chem. Soc. 89 (2012) 609–617. doi:10.1007/s11746-011-1944-3.

[14] A.D. Dinsmore, M.F. Hsu, M.G. Nikolaides, M. Marquez, et al, Colloidosomes: Selectively permeable capsules composed of colloidal particles, Sci. Washingt. 298 (2002) 1006–9.

[15] Y.-S. Gu, E.A. Decker, D.J. McClements, Formation of colloidosomes by adsorption of small charged oil droplets onto the surface of large oppositely charged oil droplets, Food Hydrocoll. 21 (2007) 516–526. doi:10.1016/J.FOODHYD.2006.05.011.

[16] J. Weil, J. Bolton, Basic Principles of Paramagnetic Resonance, in: Electron Paramagn. Reson., 2006: pp. 1–35.

[17] A. Pegi, K. Julijana, P. Slavko, Š. Janez, Š. Marjeta, The Effect of Lipophilicity of Spin-Labeled Compounds on Their Distribution in Solid Lipid Nanoparticle Dispersions Studied by Electron Paramagnetic Resonance, J. Pharm. Sci. 92 (2003) 58–66. doi:10.1002/JPS.10277.

[18] K. Jores, W. Mehnert, K. Mäder, Physicochemical investigations on solid lipid nanoparticles and on oil-loaded solid lipid nanoparticles: A nuclear magnetic resonance and electron spin resonance study, Pharm. Res. 20 (2003) 1274–1283. doi:10.1023/A:1025065418309.

[19] S. Raithore, D.G. Peterson, Effects of polyol type and particle size on flavor release in chewing gum, Food Chem. 253 (2018) 293–299. doi:10.1016/J.FOODCHEM.2018.01.123.

[20] R. V. Potineni, D.G. Peterson, Influence of Flavor Solvent on Flavor Release and Perception in Sugar-Free Chewing Gum, J. Agric. Food Chem. 56 (2008) 3254–3259. doi:10.1021/jf072783e.

[21] R. V. Potineni, D.G. Peterson, Influence of flavor solvent on flavor release and

perception in sugar-free chewing gum, J. Agric. Food Chem. 56 (2008) 3254–3259. doi:10.1021/jf072783e.

[22] D.J. Mcclements, Protein-stabilized emulsions, Curr. Opin. Colloid Interface Sci. 9 (2004) 305–313. doi:10.1016/j.cocis.2004.09.003.

[23] C.C. Berton-carabin, J.N. Coupland, C. Qian, D.J. Mcclements, R.J. Elias, Reactivity of a lipophilic ingredient solubilized in anionic or cationic surfactant micelles, Colloids Surfaces A Physicochem. Eng. Asp. 412 (2012) 135–142. doi:10.1016/j.colsurfa.2012.07.029.

[24] R.T. Rosenberg, N.R. Dan, Diffusion through colloidosome shells, J. Colloid Interface Sci. 354 (2011) 478–482. doi:10.1016/j.jcis.2010.11.011.

5. Effect of fatty acid tail-packing on the distribution and reactivity of a model hydrophobic ingredient in liposomal vesicles

5.1. Abstract

Liposomal nanovesicles were made with either saturated (80H or 90H) and unsaturated (PC75 or 90G). To investigate the effect of guest molecules in the lipid bilayer, a carrier lipid (refined coconut oil) was added at 0, 0.5, or 1.0% before homogenization. Liposome's particle size and zeta potential were characterized by dynamic light scattering and phase analysis light scattering, respectively. All nanovesicles increased in particle size with increasing carrier lipid fraction ($p < 0.05$). Zeta potential differed by phospholipid ($p < 0.05$); however, all liposomes had a negative voltage. 80H-stabilized nanovesicles become more negative with the addition of carrier lipid ($p < 0.05$). Nanovesicles made with saturated phospholipids had crystallization onset at ca. 53°C and extended from 45°C to 43°C with the addition of carrier lipid. To study distribution and reactivity, a model hydrophobic ingredient, 4-phenyl-2,2,5,5-tetramethyl-3-imidazoline-1-oxyl nitroxide (PTMIO), was used for analysis by electron paramagnetic resonance spectroscopy. Carrier lipid fraction did not affect diffusion of PTMIO in saturated or unsaturated phospholipids ($p > 0.05$). Reduction of PTMIO in 90H-stabilized liposomes was slower than other phospholipids ($p < 0.05$).

5.2. Introduction

Food, cosmetic, and drug industries often use hydrophobic ingredients to add functionality. Because many of these ingredients are hydrophobic, delivery systems are used to incorporate these compounds into aqueous systems to improve their stability and performance. Also, delivery systems are needed for active ingredients of varying hydrophilicities [1]. There has been considerable interest in developing nanoparticles, i.e., particles that are smaller than 200 nm in diameter, for the potential increase the bioavailability of active ingredients [2]. Liposomal vesicles systems, or nanovesicles, can be formed by high-pressure homogenization [3]. They can assume different structures based on the ingredients added to make the nanovesicle structure and hydrophobic ingredients incorporated into the bilayer by the method of homogenization used [1]. Liposomes were first used as a delivery system in the cosmetic industry in 1986 by Dior [4]. Nanovesicles have since been used for delivery of active compounds such as essential oils [5], antioxidants [6], and drugs [7].

The use of nanovesicles can be advantageous in the delivery of both hydrophobic and hydrophilic active ingredients. On the other hand, particle size of nanovesicles has an inverse relationship with encapsulation efficiency [8]. Further, long term stability of nanovesicles loaded with active ingredients is challenging because transport of ingredients out of the nanovesicles can occur (i.e., leaky nanovesicles) [1].

The presence of impurities in a nanovesicle's bilayer affect the characteristics of the membrane, e.g., the curvature and fluidity [9]. Lipid carriers, such as cholesterol, can be added to nanovesicles to increase the cohesion of the hydrophobic phase within nanovesicles [10]. The addition of carrier lipids is observed by a decrease in onset temperature and enthalpy in DSC [11]. However, carrier lipids and active hydrophobic ingredients will compete for space in the

nonpolar region, which can cause hydrophobic ingredients with polar moieties to be excluded from the region [12].

The zeta potential of nanovesicles is mainly determined by the hydrophilic head group, but is also affected by the presence of impurities (i.e., structural or active encapsulated compounds) [13]. The zeta potential of empty nanovesicles, i.e., nanovesicles made without any encapsulant, be a lesser negative value than that of similar nanovesicles with an encapsulated ingredient [7]. With the addition of guest molecules into the nanovesicles can cause a change in the orientation of the headgroup of the lecithin [7].

The permeability of nanovesicles is determined by the fatty acid profile of the phospholipid [13]. Permeability of nanovesicles is often measured as the lipid phase transition by differential scanning calorimetry (DSC). The transition temperature is lowered by decreasing the chain length and adding unsaturations of the fatty acid chain [9]. Because of unsaturations in the fatty acid tails, increasing the carrier lipid concentration will decrease the release rate of carried ingredients. On the other hand, lecithins with saturated fatty acid tails form more rigid membranes in nanovesicles [10].

One way to measure the performance of a delivery system is by the distribution and reactivity of an encapsulated model ingredient *in-situ*. Electron paramagnetic resonance (EPR) spectroscopy is a technique that is based on aligning unpaired electrons in an applied magnetic field. EPR spin labeling, i.e., using a stable nitroxide radical, has been used to characterize the distribution of a model hydrophobic molecule's distribution in emulsions [14,15] and surfactant micelles [16]. Further, EPR can follow the distribution of spin probes, *in-situ* [14]. The use of EPR-active spin-probes to investigate the dynamics in the nanovesicle bilayer does not affect the

internal structure of nanovesicles [17]. The addition of carrier lipid can be serendipitous in understanding the bilayer behavior both by DSC and EPR.

The objective of the current study was to understand how saturated and unsaturated phospholipids encapsulate hydrophobic molecules at different levels of carrier lipid, using an EPR-active spin probe as a model ingredient. Further, to characterize the packing of the fatty acid tails of lecithin with increasing carrier lipid content and to characterize the distribution, release kinetics, and reactivity of the model hydrophobic ingredient with EPR spectroscopy.

5.3. Materials and methods

5.3.1. Materials

Sodium ascorbate, ferric chloride, and sodium caseinate were procured from Alfa Aesar (Ward Hill, MA). The EPR-active spin probe, 4-phenyl-2,2,5,5-tetramethyl-3-imidazoline-1-oxyl nitroxide (PTMIO) was purchased from Enzo Life Sciences with (>95% purity; Plymouth Meeting, MI). Refined coconut oil (i.e., composed of 50% caprylic and 50% capric acid as determined by methyl ester analysis) was purchased from a local grocery store. Lipoid P75 (PC75; phospholipids from soybean with 68-73% phosphatidylcholine, 10% lysophaphatidylcholine, and 5-10% phosphatidylethanolamine), Phospholipon 90H (90H; hydrogenated soybean phospholipids with 90% phosphatidylcholine), Phospholipon 90G (90G; phospholipids from soybean with 94% phosphatidylcholine and 4% lysophaphatidylcholine), and Phospholipon 80H (80H; hydrogenated soybean phospholipids with 70% phosphatidylcholine) were purchased from The American Lecithin Company (Newark, NJ). All chemicals were analytical grade and used without further modification.

5.3.2. Preparation of liposomal vesicles

PC75, 90H, 90G, and 80H lecithins (4 wt%) were dispersed in water at 60°C on a magnetic stir plate for 1 h. PTMIO was added 200 μM (21.7 ppm) to the premix. Refined coconut oil was added at 0, 0.5, and 1.0 wt% to the premix. Crude homogenization by high shear mixing (Ika Works; Wilmington, NC) was done at 24,000 rpm for 1 min. Fine homogenization was done in a 2-stage homogenizer (Panda Plus 2000, GEA Niro Soavi; Parma, Italy) at 60-65°C, 500 bar (where the second stage is set to 50 bar and the total pressure is set to 500 bar with the first stage), for 3 passes. Prepared liposomes were stored at refrigeration temperature (4°C) until further analysis.

5.3.3. Particle size and zeta potential analysis

Liposomal vesicles were characterized for their particle size and zeta potential in a DelsaMax Pro with a flow cell attachment and assist unit (Beckman Coulter; Brea, CA). Reported values for particle size are the volume-surface mean (d_{32}). Zeta potential was measured with a refractive index of 1.33 at 20°C. Liposomal vesicles were dilute 1:500 in water for particle size and zeta potential analysis to avoid multiple scattering effects.

5.3.4. EPR analysis

The distribution and reactivity of the particles were assessed by using a spin labeling EPR technique described in our previous works (REF). Briefly, nanovesicles containing PTMIO (200 μmol L^{-1}) was deoxygenated with humified N_2 gas for 15 min (ca. 3 L min^{-1}). Then, aliquots of samples (50 μL) were loaded in a borosilicate capillary tubes (Leica Microsystems, Wetzlar, Germany), sealed with vinyl plastic putty for subsequent EPR analysis. EPR measurements were conducted at room temperature in an EPR spectrometer operating at X-band (SpinscanX, Adani;

Minsk, Belarus). The measurement conditions were 335.5 mT center field, 6.0 mT sweep width, 100kHz modulation frequency, 100 uT modulation amplitude, and 6.3 mW microwave power. Multicomponent EPR spectra were simulated using the WinSim2002 program (version 0.98, National Institute of Environmental Health Sciences, NIH; Bethesda, MD) to deconvolute signals of PTMIO in environments with distinct polarities [14,18]. Hyperfine coupling constants, a_N, and rotational correlation time τ_c(C) provide insights to the polarity and mobility that PTMIO experiences [19].

5.3.5. Reactivity of the model ingredient

An ascorbate assay was used to study the reactivity of PTMIO *in situ*. Briefly, 1 mmol kg^{-1} sodium ascorbate and 10 μmol kg^{-1} ferric chloride was added to 100 mL of each of the liposomal vesicles. Within 30 s of adding all of the reactants, liposomal vesicles were loaded into glass micropipettes, sealed, and placed into the EPR cavity. EPR spectra were collected every 2 min for the first 30 min of the reaction. With the addition of ascorbate, PTMIO is reduced to an EPR-silent form. Because ascorbate is polar (log *P* = -1.85), it only depletes PTMIO in the aqueous phase [15]. Reaction progress of ascorbate was quantified as the first order kinetics reaction rate constant (k value).

5.3.6. DSC analysis

The thermal properties of the nanovesicles were determined using a Q2000 DSC (TA instruments, New Castle, DE, USA) for the onset temperature, peak height, and enthalpy of crystallization and melting. Aliquots of nanovesicle dispersions (ca. 10 mg) were loaded into a hermetically sealed DSC pan. An empty pan was used as a reference. The DSC experiment

include heating (20–95°C) and cooling (95-2°C) of the pans at a rate of 5°C min^{-1}. All samples were analyzed by DSC within 48 h from homogenization.

5.3.7. Statistical analysis

All measurements are the average of 4 replicates unless otherwise reported. The effects of lecithin type and carrier lipid fraction on the particle size, zeta potential, rotational correlation time, and k-values were analyzed by analysis of variance (ANOVA) with a general linear model. Tukey's post comparison test was applied to see differences between treatments. Significance was considered at ($p < 0.05$). Statistical analysis was performed in Minitab v17 (State College, PA).

5.4. Results and discussion

5.4.1. Physical properties of liposomal vesicles

To determine the homogenization conditions to use for nanovesicles in the study, PC75 was processed by crude homogenization (high shear mixing only), high shear mixing and high-pressure homogenization in a two-stage homogenizer at 100 bar, or crude homogenization and high-pressure homogenization at 500 bar (Figure A.5). High shear mixing alone produced the largest particle size. When comparing nanoparticles made with 100 and 500 bar, the variability is similar. 500 bar was selected because it gave the smallest particle size.

Nanovesicles were characterized for particle size and zeta potential immediately following homogenization. The particle size of the nanovesicles with no carrier lipid were all smaller than 100 nm and did not differ by lecithin type ($p > 0.05$; Figure 5.1). The addition of 0.5% carrier lipid did not increase the particle size from 0% carrier lipid ($p > 0.05$). With respect to the liposomes made with no carrier lipid, addition of 1.0% carrier lipid increased the particle

size. Both saturated lecithins (90H and 80H) have an increase in particle size from 0% to 1.0% carrier lipid. Interestingly, further addition of carrier lipid did not affect the particle size of 90G-stabilized liposomes from 0.5% to 1.0%. When comparing the particle size of liposomes made by two unsaturated lecithins (PC75 and 90G), the 90G lecithin formulation has some 20% more phosphatidylcholine, which may better incorporate the larger carrier lipid fraction into nanovesicles. The addition lipids to the liposome membrane can increase the particle size of the formed liposomes [20]. The increase in particle size may be attributed to the decrease in membrane curvature [21].

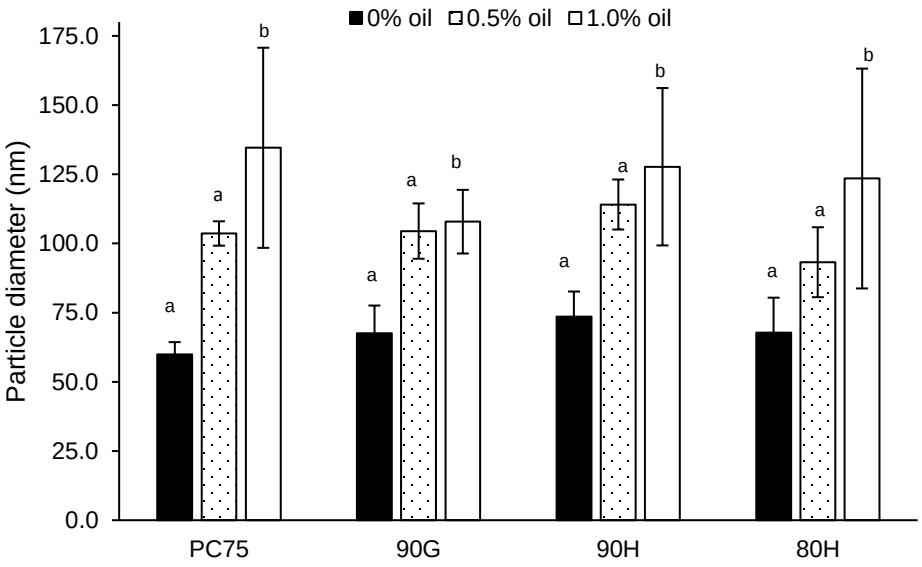

Figure 5.1. Volume-surface mean diameter (d_{32}) of liposomal vesicles made with either PC75, 90G, 90H, or 80H lecithins at carrier lipid fractions of 0%, 0.5%, 1.0% refined coconut oil. Error bars represent the standard deviation. Letters show significant differences between oil fractions at ($p < 0.05$).

PC75-stabilized liposomes have a greater negative value than other lecithins, all lecithin and carrier lipid combinations had a zeta potential between 0 and -20 mV (Figure 5.2). For PC75, 90G, and 90H lecithins, the zeta potential does not change when carrier lipid is added. On

the other hand, the zeta potential of 80H lecithin becomes more negative with the addition of carrier lipids ($p < 0.05$; Figure 5.2). A similar pattern to 80H in this study was observed with in egg phosphatidylcholine-stabilized liposomes loaded with a drug with drugs with increasing hydrophobicity [7]. The change in zeta potential of 80H liposomes with carrier lipid may be due to a change in the orientation of the head group of the phospholipid at the surface.

5.4.2. Thermal properties of nanovesicles

Crystallization of fatty acid tail in nanovesicles were observed as exothermic peaks in DSC thermograms (Figure 5.3). Neither nanovesicles made with unsaturated (PC75 and 90G) lecithins nor their lecithin powders displayed phase transitions on -40°C to 100°C (data not shown). Nanovesicles made with saturated (90H and 80H) saw an insignificant decrease in onset temperature, peak height, and enthalpy of crystallization ($p > 0.05$; Table 1). Although insignificant in this study, the observation is consistent with previous findings [11]. The addition of guest molecules into the bilayer can change the orientation of the fatty acid tail [22], such as a change from *trans*- to *gauche*- orientation [23]. As the fraction of carrier lipid increases, the fatty acid tails closer of the phospholipid are moved to the nanovesicle's surface. On the other hand, the presence of a guest molecule in the bilayer could interfere with the orientation of a lecithin's fatty acid tail to orient with similar molecules [12]. Nanovesicles in this study had an excipient carrier lipid added, which is expected to associate with the lecithin's fatty acid tails and not near the polar moiety. Although, for EPR analysis, the spin probe added may orient at the nanovesicle surface which would disrupt the nanovesicle surface. However, the presence of PTMIO didn't affect the thermal properties of nanovesicles. Other researchers observed similar behavior of PTMIO in lecithin bilayers [14].

Table 5.1. Onset temperature, peak maximum, and enthalpy of 90H and 80H lecithin powders and liposomal vesicles at 0%, 0.5%, and 1.0% carrier lipid.

Lecithin	Parameter	Powder	0% oil	0.5% oil	1.0% oil
	onset (°C)	82.72 ± 0.82[a]	54.81 ± 0.68[b]	54.49 ± 1.69[b]	53.46 ± 2.64[b]
90H	peak (W mmol^{-1})	5.33 ± 1.55[a]	7.05 ± 0.25[a]	6.56 ± 1.10[a]	4.93 ± 4.93[a]
	ΔH (W mmol^{-1})	711.70 ± 320.17[a]	5.77 ± 1.51[b]	2.81 ± 0.48[b]	2.07 ± 0.48[b]
	onset (°C)	81.43 ± 1.60[a]	53.84 ± 3.0[b]	53.63 ± 4.24[b]	52.64 ± 4.48[b]
80H	peak (W mmol^{-1})	5.52 ± 1.96[a]	4.20 ± 0.93[a]	4.76 ± 1.16[a]	3.43 ± 0.47[a]
	ΔH (W mmol^{-1})	308.66 ± 108.20[a]	3.06 ± 2.64[b]	2.29 ± 1.92[b]	1.47 ± 0.72[b]

Different connecting letters show significant differences within onset temp., peak maximum, or enthalpy at ($p > 0.05$).

5.4.3. Location of the model hydrophobic ingredient in liposomes

EPR spectroscopy was used to evaluate the distribution and mobility of hydrophobic ingredients in nanovesicles. A model hydrophobic ingredient, PTMIO, was selected for its tendency to associate in lipid environments, based on its log *P* value of 2.5. PTMIO is expected to behave similar to hydrophobic ingredients in food, drug, and cosmetic applications.

PTMIO in liposomes creating showed a typical nitroxide triplet signal with distinct hyperfine splitting constants (a_N; Figure 5.4). EPR Spectra were deconvoluted for their a_N and fractions fraction in either the aqueous or lipid phase by a simulation technique that has been used to separate PTMIO in unique chemical environments in emulsions [14] and micelles [24]. Spectra of the simulations are superimposed with their respective unprocessed spectra (Figure 5.4).

In liposomes made with PC75 lecithin without a carrier lipid, the aqueous fraction of PTMIO in both lecithins have a a_N of 1.64 mT and of 1.66 mT in the lipid phase the addition of

carrier lipid to PC75 liposomes does not affect the a_N of the system. The a_N of 90G and 80H also did not change with increasing carrier lipid content. Although, 90H liposomes have a a_N of 1.63 mT, 1.64 mT, and 1.66 mT at 0%, 0.5%, and 1.0% carrier lipid fraction, respectively.

τ_c(C) was calculated for PTMIO in the lipid fraction of nanovesicles (Table 1). PC75 nanovesicles had a greater. τ_c(C) than nanovesicles made with other lecithins ($p < 0.05$). Nanovesicles made with 1.0% carrier lipid had greater τ_c(C) than nanovesicles made with 0 or 0.5% carrier lipid ($p < 0.05$). The addition of carrier also disrupted the crystallization of nanovesicles made with saturated lecithins, as observed by DSC. This may cause greater mobility within the nanovesicles membrane with a higher carrier lipid fraction is the increase in fluidity. Previous investigation of a spin probe loaded into phospholipid liposomes had limited mobility [25]. The addition of guest molecules interrupts the organization of the lipid bilayer, which increases the mobility of molecules within the bilayer [26]. Indeed, with the τ_c(C) of 0% carrier lipid PC75 nanovesicles is increased ca. 10-fold with the addition of either 0.5% or 1.0% carrier lipid (Table 2).

5.4.4. Reactivity of the model hydrophobic ingredient in liposomes

To understand the reactivity and transport of encapsulated hydrophobic ingredients in liposomes *in situ,* PTMIO was reduced to an EPR-silent form by an ascorbate assay. Reaction progress was monitored for the first 30 minutes after the addition of ascorbate to the liposomes (Figure 5.5). Because ascorbate is polar, it reacts with PTMIO in the aqueous region and interface, PTMIO in the lipid phase is not expected to react with ascorbate [14].

Reaction rate constants (k values) are reported as the first order reaction rate constants (Table 3). In nanovesicles made with unsaturated lecithins (PC75 and 90G) was similar with 0%

carrier lipid addition ($p > 0.05$). At 0.5% and 1.0% carrier lipid, unsaturated lecithins also did not have different k values ($p > 0.05$). Because neither unsaturated lecithin displayed crystallization events by DSC analysis, unsaturated nanovesicles are expected to be largely fluid. PTMIO in PC75 nanovesicles had greater mobility, but this did not correlate with the k value. PTMIO has been previously shown to react more quickly with anionic micelles than cationic micelles [24]. 90G nanovesicles with carrier lipid were expected to have a greater negative zeta potential, however this was not observed in the present study. Further the partitioning behavior of PTMIO in the lipid phase of nanovesicles made with unsaturated lecithins was similar at each carrier lipid fraction (Table 4).

For nanovesicles made with saturated lecithins, 80H nanovesicles were not different from unsaturated (PC75 or 90G) nanovesicles ($p > 0.05$). On the other hand, 90H had a lesser reaction rate ($p < 0.05$; Table 3). One explanation for the difference is by the crystallization nature of the bilayer. Because 90H has greater crystallization enthalpies at all carrier lipid fraction, 90H nanovesicle membrane may less disrupted than 80H nanovesicles (Table 2). PTMIO in 90H nanovesicles is largely excluded from the lipid phase at 0 and 0.5% carrier lipid (Table 4). With the addition of carrier lipid at both fractions, the zeta potential of 80H nanovesicles becomes a greater negative value (Figure 5.2). The zeta potential of nanovesicles did not affect the reaction rate of nanovesicles made with unsaturated lecithins. However, the zeta potential 80H nanovesicles is a greater negative value than 90H. The addition of guest molecules can affect the zeta potential of the liposomes, possibly by changing the head group orientation [7]. Changing the charge of the overall liposomes could change the location of PTMIO in the liposome, such as the orientation of resveratrol in cationic and zwitterionic liposomes [6]. Although, the fraction of

PTMIO in the lipid fraction of 80H nanovesicles is ca. 20% greater than 90H nanovesicles (Table 4).

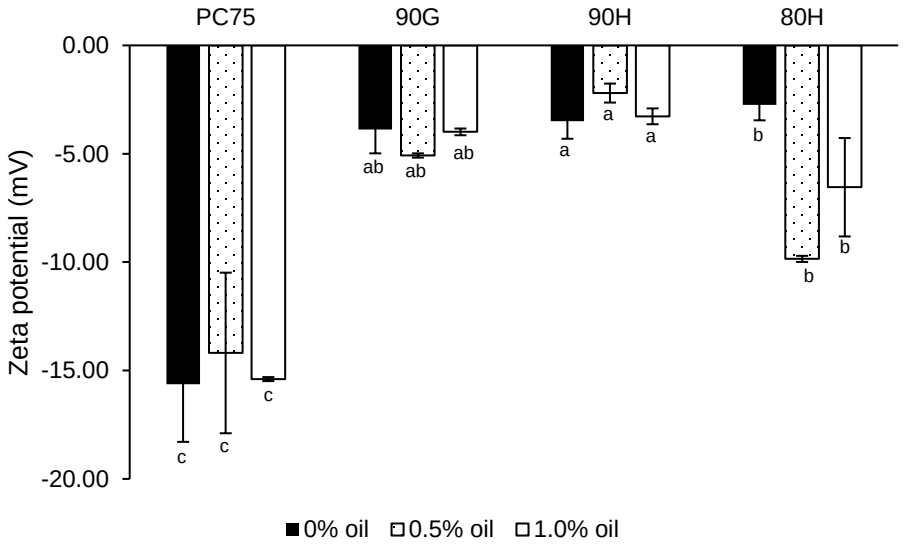

Figure 5.2. Zeta potential of liposomal vesicles made with either PC75, 90G, 90H, or 80H lecithins at carrier lipid fractions of 0%, 0.5%, 1.0% refined coconut oil. Conditions with different connecting letters are significantly different from other lecithin types at ($p < 0.05$).

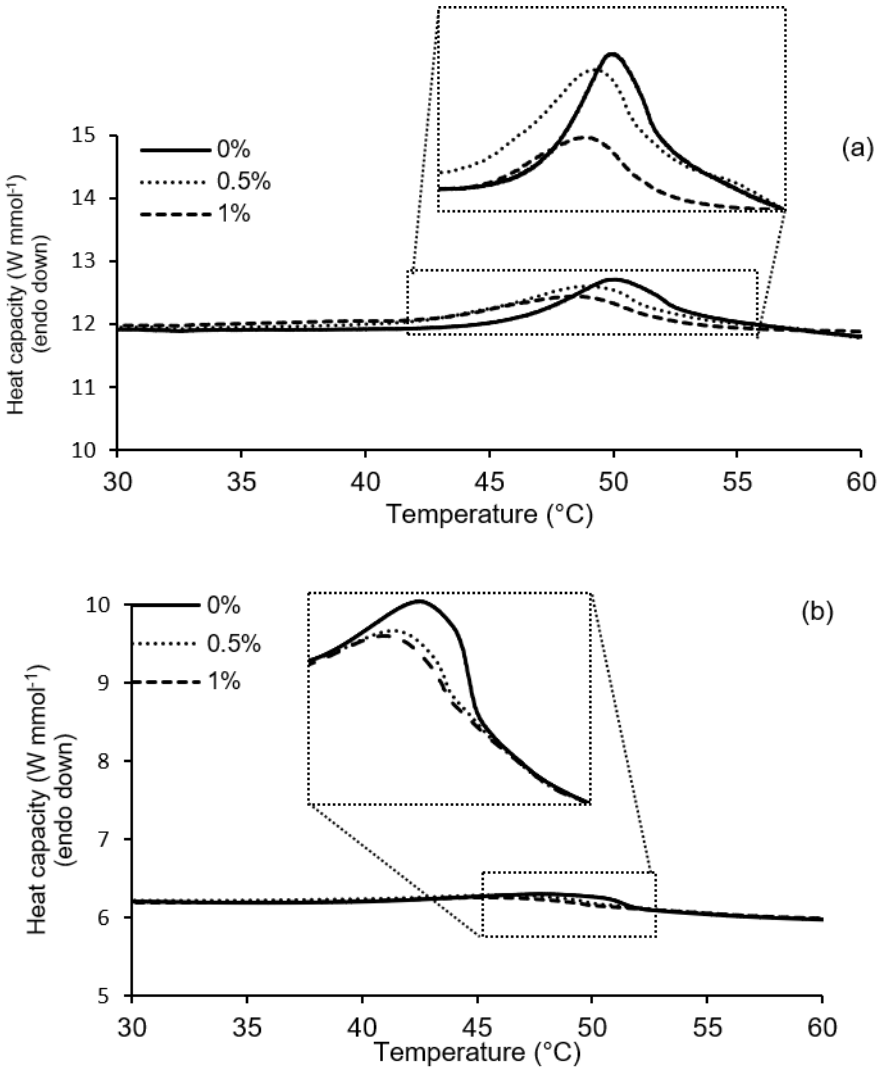

Figure 5.3. DSC cooling thermograms of 90H (a) and 80H (b) liposomal vesicles at carrier lipid fractions of 0%, 0.5%, 1.0% refined coconut oil. The scale of the y-axis reflects the scale of the bottom cooling curve.

Table 5.2. Rotational correlation time (τ_c(C)) values of PTMIO in nanovesicles stabilized with PC75, 90G, 90H, or 80H lecithins.

	τ_c(C) ($\times 10^{13}$; s)		
Lecithin	0%	0.5%	1.0%
PC75	0.87 ± 1.42^{a}	10.93 ± 3.29^{a}	11.60 ± 2.16^{a}
90G	9.92 ± 1.72^{ab}	3.32 ± 3.80^{ab}	9.86 ± 4.30^{ab}
90H	3.16 ± 1.01^{ab}	7.06 ± 2.45^{ab}	8.82 ± 2.14^{ab}
80H	5.22 ± 2.06^{b}	5.37 ± 3.29^{b}	6.74 ± 1.42^{b}

Values are the average of four replicates ± standard deviation of 2 replicates. Different letters show significant differences between lecithin types at ($p < 0.05$).

Table 5.3. First order Reaction rate constants, k (min-1), of PTMIO reduction by ascorbate in liposomal vesicles at carrier lipid fractions of 0%, 0.5%, and 1.0%.

	k (min^{-1}; $\times 10^{-3}$)		
Lecithin	0% oil	0.5% oil	1.0% oil
PC75	7.41 ± 1.05^{ab}	6.08 ± 0.50^{ab}	6.49 ± 0.77^{ab}
90G	6.39 ± 2.82^{ab}	6.34 ± 2.78^{ab}	5.84 ± 2.70^{ab}
90H	4.09 ± 1.05^{b}	3.75 ± 0.39^{b}	3.60 ± 0.56^{b}
80H	7.47 ± 1.56^{a}	6.51 ± 2.78^{a}	6.55 ± 1.84^{a}

Values are means ± standard deviation of 4 replicates. Different connecting letters show differences between lecithin types at ($p < 0.05$).

Table 5.4. Fractions of PTMIO in the lipid of fraction of liposomal vesicles stabilized with PC75, 90G, 90H, or 80H lecithins during an ascorbate assay.

	PC75 lecithin			90G lecithin		
Time (min)	0% oil	0.5% oil	1.0% oil	0% oil	0.5% oil	1.0% oil
0	38.8 ± 4.0^{a}	40.0 ± 1.4^{a}	46.8 ± 6.7^{a}	59.3 ± 5.8^{a}	57.2 ± 3.3^{a}	42.1 ± 3.7^{a}
9	58.5 ± 8.5^{b}	45.8 ± 8.2^{a}	49.3 ± 4.9^{a}	67.8 ± 5.0^{a}	50.5 ± 8.4^{a}	53.9 ± 12.1^{a}
19	74.3 ± 5.0^{c}	62.5 ± 9.3^{a}	45.5 ± 1.7^{a}	68.1 ± 4.5^{a}	63.1 ± 7.5^{a}	48.9 ± 4.8^{a}
	90H lecithin			80H lecithin		
Time (min)	0% oil	0.5% oil	1.0% oil	0% oil	0.5% oil	1.0% oil
0	23.4 ± 16.4^{a}	21.8 ± 17.2^{a}	62.0 ± 8.6^{a}	47.2 ± 3.8^{a}	58.3 ± 2.6^{a}	49.0 ± 10.2^{a}
9	20.9 ± 2.5^{ab}	13.6 ± 3.9^{a}	65.5 ± 8.9^{a}	38.3 ± 6.4^{a}	56.2 ± 2.6^{a}	54.3 ± 2.5^{a}
19	7.4 ± 3.7^{b}	19.6 ± 11.4^{a}	54.3 ± 8.9^{a}	42.8 ± 4.4^{a}	25.9 ± 9.3^{b}	61.1 ± 3.2^{a}

Values are the average of four replicates ± standard deviation of 4 replicates. Different connecting letters show differences with a lecithin type at an oil fraction at ($p < 0.05$).

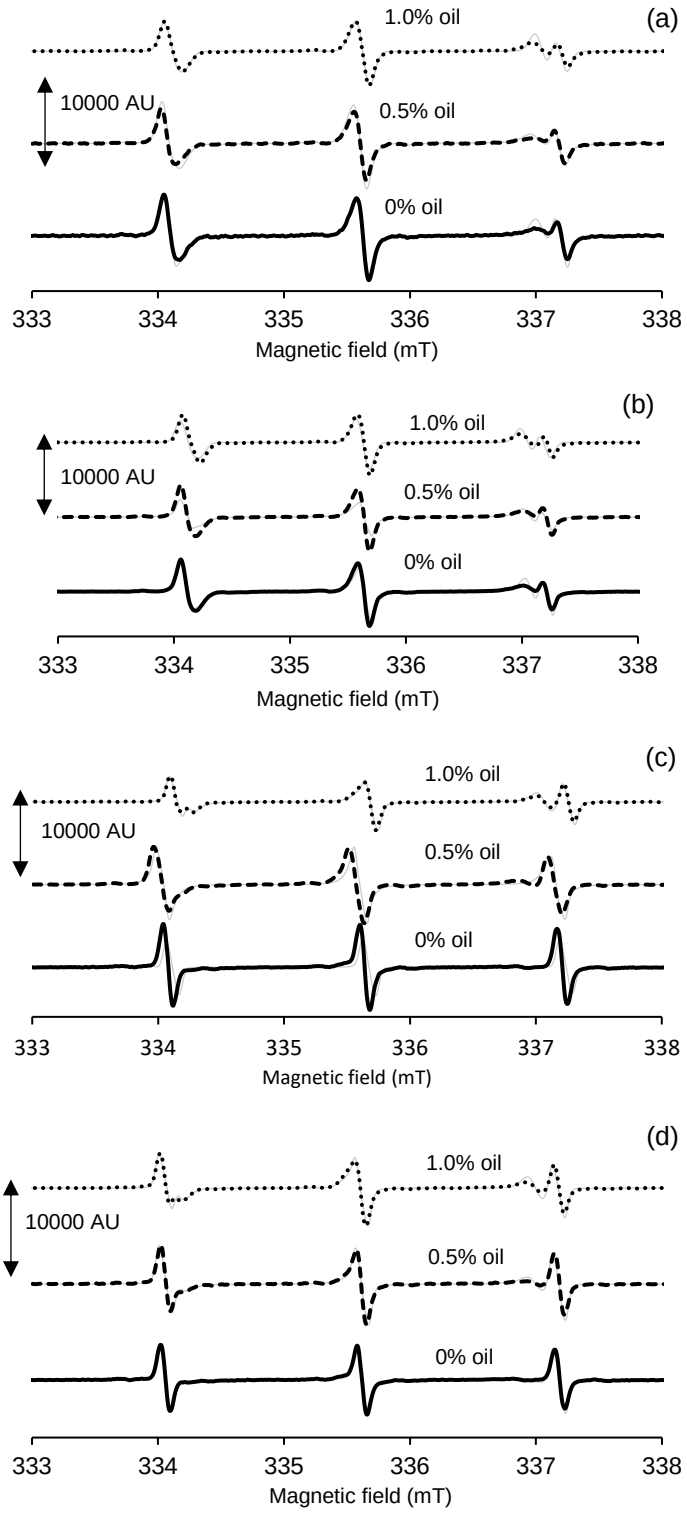

Figure 5.4. Typical EPR spectra and simulation of PTMIO in liposomal vesicles made with either PC75 (a), 90G (b), 90H (c), or 80H (d) at carrier lipid fractions of 0%, 0.5%, 1.0% refined coconut oil.

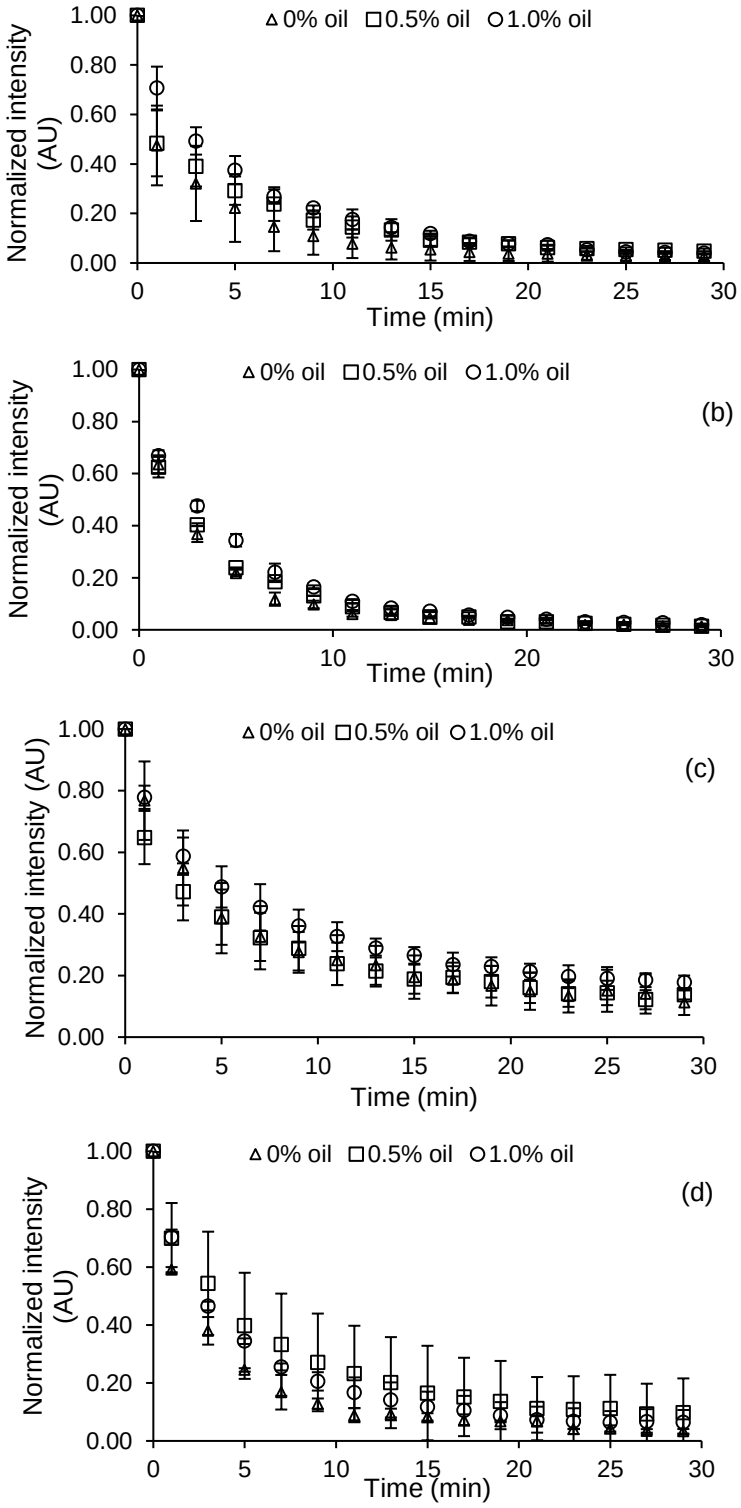

Figure 5.5. Reaction progress of PTMO reduction by ascorbate in liposomal vesicles made with either PC75 (a), 90G (b), 90H (c), or 80H (d) at carrier lipid fractions of 0%, 0.5%, 1.0% refined coconut oil.

5.5. Conclusion

Nanovesicles were formed with saturated and unsaturated phospholipids with different levels of carrier lipid. Unsaturated PC75 and both saturated (90H and 80H) phospholipids increased in particle size with the addition of 1.0% carrier lipid, whereas unsaturated 90G did not increase in particle size with that carrier lipid fraction. A model ingredient in nanovesicles made with 90H saturated lecithin had lesser reactivity than unsaturated lecithins. Although a model ingredient also reacted faster in saturated 80H nanovesicles, the addition ingredients may change the interaction of the lecithin head group. Active molecules loaded into saturated lecithins may be useful for applications where prolonged release is desirable. To further extend release of ingredients from nanovesicles, the addition of a solid fat to nanovesicles should be investigated as to whether hydrophobic ingredients are excluded from the lipid soluble region.

5.6. References

[1] A. Sharma, U.S. Sharma, Liposomes in drug delivery: progress and limitations Amarnath, Int. J. Pharm. 154 (1997) 123–140.

[2] E. Acosta, Bioavailability of nanoparticles in nutrient and nutraceutical delivery, Curr. Opin. Colloid Interface Sci. 14 (2009) 3–15. doi:10.1016/j.cocis.2008.01.002.

[3] D Bachmann, Preparation of liposomes using a mini-lab 8.30 H high-pressure homogenizer, Int. J. Pharm. 91 (1993) 69–74.

[4] R.H. Müller, K. Mader, S. Gohla, Solid lipid nanoparticles (SLN) for controlled drug delivery - review of the state of the art, Eur. J. Pharm. Biopharm. 50 (2000) 161–177. doi:10.1016/s0928-0987(97)86243-4.

[5] Z. Wen, X. You, L. Jiang, B. Liu, Z. Zheng, Y. Pu, B. Cheng, Liposomal incorporation of rose essential oil by a supercritical process, Flavour Fragr. J. 26 (2011) 27–33. doi:10.1002/ffj.2012.

[6] C. Bonechi, S. Martini, L. Ciani, S. Lamponi, H. Rebmann, C. Rossi, S. Ristori, Using liposomes as carriers for polyphenolic compounds: The case of Trans-resveratrol, PLoS One. 7 (2012). doi:10.1371/journal.pone.0041438.

[7] D.G. Fatouros, S.G. Antimisiaris, Effect of amphiphilic drugs on the stability and zeta-potential of their liposome formulations: A study with prednisolone, diazepam, and griseofulvin, J. Colloid Interface Sci. 251 (2002) 271–277. doi:10.1006/jcis.2002.8432.

[8] B. Lohse, P.Y. Bolinger, D. Stamou, Encapsulation efficiency measured on single small unilamellar vesicles, J. Am. Chem. Soc. 130 (2008) 14372–14373. doi:10.1021/ja805030w.

[9] M.R. Mozafari, C. Johnson, S. Hatziantoniou, C. Demetzos, Nanoliposomes and their applications in food nanotechnology, J. Liposome Res. 18 (2008) 309–327. doi:10.1080/08982100802465941.

[10] C. Demetzos, Differential Scanning Calorimetry (DSC): A tool to study the thermal behavior of lipid bilayers and liposomal stability, J. Liposome Res. 18 (2008) 159–173. doi:10.1080/08982100802310261.

[11] C. Matsingou, C. Demetzos, Calorimetric study on the induction of interdigitated phase in hydrated DPPC bilayers by bioactive labdanes and correlation to their liposome stability. The role of chemical structure, Chem. Phys. Lipids. 145 (2007) 45–62. doi:10.1016/j.chemphyslip.2006.10.004.

[12] C. Matsingou, C. Demetzos, The perturbing effect of cholesterol on the interaction between labdanes and DPPC bilayers, Thermochim. Acta. 452 (2007) 116–123. doi:10.1016/j.tca.2006.10.015.

[13] D.J. McClements, Encapsulation, protection, and release of hydrophilic active components: Potential and limitations of colloidal delivery systems, Adv. Colloid Interface Sci. 219 (2015) 27–53. doi:10.1016/j.cis.2015.02.002.

[14] U. Yucel, R.J. Elias, J.N. Coupland, Solute distribution and stability in emulsion-based delivery systems: An EPR study, J. Colloid Interface Sci. 377 (2012) 105–113. doi:10.1016/j.jcis.2012.03.071.

[15] C.C. Berton-Carabin, J.N. Coupland, R.J. Elias, Effect of the lipophilicity of model ingredients on their location and reactivity in emulsions and solid lipid nanoparticles, Colloids Surfaces A Physicochem. Eng. Asp. 431 (2013) 9–17.

doi:10.1016/j.colsurfa.2013.04.016.

[16] C.C. Berton-carabin, J.N. Coupland, C. Qian, D.J. Mcclements, R.J. Elias, Reactivity of a lipophilic ingredient solubilized in anionic or cationic surfactant micelles, Colloids Surfaces A Physicochem. Eng. Asp. 412 (2012) 135–142. doi:10.1016/j.colsurfa.2012.07.029.

[17] G. Martini, L. Ciani, Electron spin resonance spectroscopy in drug delivery, Phys. Chem. Chem. Phys. 11 (2009) 211–254. doi:10.1039/b808263d.

[18] U. Yucel, R.J. Elias, J.N. Coupland, Localization and reactivity of a hydrophobic solute in lecithin and caseinate stabilized solid lipid nanoparticles and nanoemulsions, J. Colloid Interface Sci. 394 (2013) 20–25. doi:10.1016/J.JCIS.2012.12.042.

[19] U. Yucel, R.J. Elias, J.N. Coupland, Solute distribution and stability in emulsion-based delivery systems: An EPR study, J. Colloid Interface Sci. 377 (2012) 105–113. doi:10.1016/J.JCIS.2012.03.071.

[20] S. Varona, Á. Martín, M.J. Cocero, Liposomal incorporation of lavandin essential oil by a thin-film hydration method and by particles from gas-saturated solutions, Ind. Eng. Chem. Res. 50 (2011) 2088–2097. doi:10.1021/ie102016r.

[21] M.A. Vélez, M.C. Perotti, P. Zanel, E.R. Hynes, A.M. Gennaro, Soy PC liposomes as CLA carriers for food applications: Preparation and physicochemical characterization, J. Food Eng. 212 (2017) 174–180. doi:10.1016/j.jfoodeng.2017.06.001.

[22] O.G. Mouritsen, K. Jørgensen, Dynamical order and disorder in lipid bilayers, Chem. Phys. Lipids. 73 (1994) 3–25. doi:10.1016/0009-3084(94)90171-6.

[23] D. Pentak, Physicochemical properties of liposomes as potential anticancer drugs

carriers. Interaction of etoposide and cytarabine with the membrane: Spectroscopic studies, Spectrochim. Acta - Part A Mol. Biomol. Spectrosc. 122 (2014) 451–460. doi:10.1016/j.saa.2013.11.061.

[24] C.C. Berton-Carabin, R.J. Elias, J.N. Coupland, Reactivity of a model lipophilic ingredient in surfactant-stabilized emulsions: Effect of droplet surface charge and ingredient location, Colloids Surfaces A Physicochem. Eng. Asp. 418 (2013) 68–75. doi:10.1016/j.colsurfa.2012.11.010.

[25] A. Pegi, K. Julijana, P. Slavko, Š. Janez, Š. Marjeta, The Effect of Lipophilicity of Spin-Labeled Compounds on Their Distribution in Solid Lipid Nanoparticle Dispersions Studied by Electron Paramagnetic Resonance, J. Pharm. Sci. 92 (2003) 58–66. doi:10.1002/JPS.10277.

[26] W.W. Sułkowski, D. Pentak, K. Nowak, A. Sułkowska, The influence of temperature, cholesterol content and pH on liposome stability, J. Mol. Struct. 744–747 (2005) 737–747. doi:10.1016/j.molstruc.2004.11.075.

Chapter 6 - Conclusions

There is a need to encapsulate active molecules which provide functionality to food, cosmetic, and drug applications. There has been an interest in developing delivery systems at the nanoscale for their improved stability to instabilities such as separation by gravity and an increase in surface area. To understand how active ingredients will behave in these systems, electron paramagnetic resonance (EPR) spectroscopy was used to characterize the of distribution and reactivity of model hydrophobic ingredients in these delivery systems.

A delivery system with the possibility for pH-triggered release is presented in Chapter 4. Colloidosome structures formed are colloidal aggregates formed by electrostatic deposition of oppositely charged nanoparticles. Because active ingredients in solid lipid nanoparticles (SLN) are excluded from the lipid core, the colloidosomes formed are composed of SLN which are adsorbed to the surface of a liquid lipid nanoemulsion (LLN). This chapters shows that the addition of solid shell does not change the distribution of active ingredients loaded hydrophobic ingredients but limit the diffusion of hydrophobic ingredients from the LLN core. These structures have potential to be used for preferential release of hydrophobic ingredients. These structures should be further investigated for treatments (such as sintering or enzymatic cross linking) further inhibit the diffusion and reactivity of molecules loaded into colloidosomes.

In Chapter 5, liposomal nanovesicles were formed by saturated or unsaturated lecithins with different fractions of excipient carrier lipid. When carrier lipid was added to saturated 80H lecithin, a change in the orientation of the hydrophilic headgroup of the lecithin was observed by an increase in negative zeta potential. Reactivity of a model hydrophobic ingredient is lesser in saturated 90H lecithin compared to saturated 80H or unsaturated lecithin (PC75 and 90G). A

continuation of this study should be adding a solid fat to the nanovesicles, instead of a liquid one, which could determine if hydrophobic ingredients would be expelled from nanovesicle made with solid fat and how that exclusion affected the reactivity of hydrophobic ingredients. Further if the solid fat in nanovesicles acted as a barrier, trapping aqueous substances on the nanovesicle interior, the delivery system could have potential for the delivery of hydrophilic ingredients.

Appendix A - Supplemental data

A.1. Preliminary particle size data for emulsions in Chapter four

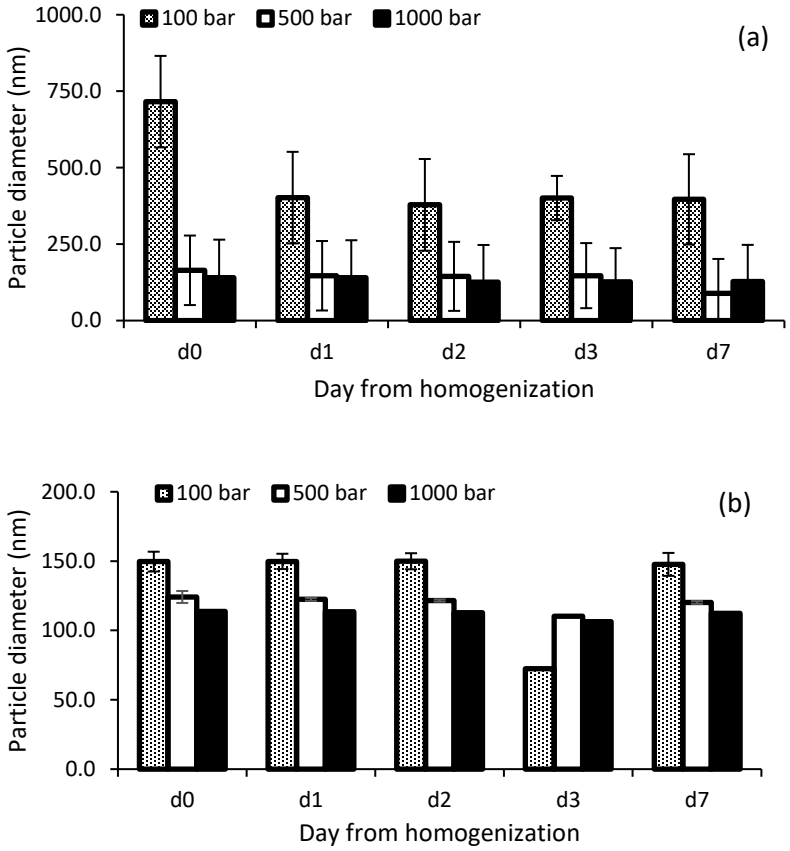

Figure A.1. d_{32} of caseinate (a) and PC75 (b) 10% oil in water emulsions prepared at 100, 500, and 1000 bar over one five days. Emulsions were prepared as described in Chapter 4.

A.2. Supplementary atmospheric pressure chemical ionization of colloidosomes loaded limonene

Atmospheric pressure chemical ionization-mass spectroscopy (APcI-MS) data was collected at the University of Minnesota by Dr. Umut Yucel. APcI-MS analysis was done using a method described by Potineni and Peterson [1]. Headspace concentration of limonene-containing emulsions in a jacketed and deactivated glass reaction vessel with hermetic injection ports equilibrated at 30 °C was continuously sampled at a sampling rate of 175 mL/min and transfer line temperature of 90°C to prevent condensation. Humidified air was supplied to prevent drying of the samples. Limonene concentration was determined by using a triple-quadruple mass spectrometer (Micromass Quattro Ultima; Waters Corporation, Milford, MA) operating at corona discharge of 3.5 kV, and cone voltage of 20 V for selected ions (m/z 67, 81, 95). A picture of the complete systems is provided as a supplementary material. An image of the vessel used is proved (Figure A.2). A summary of the findings of limonene release is illustrated in Figure A.3.

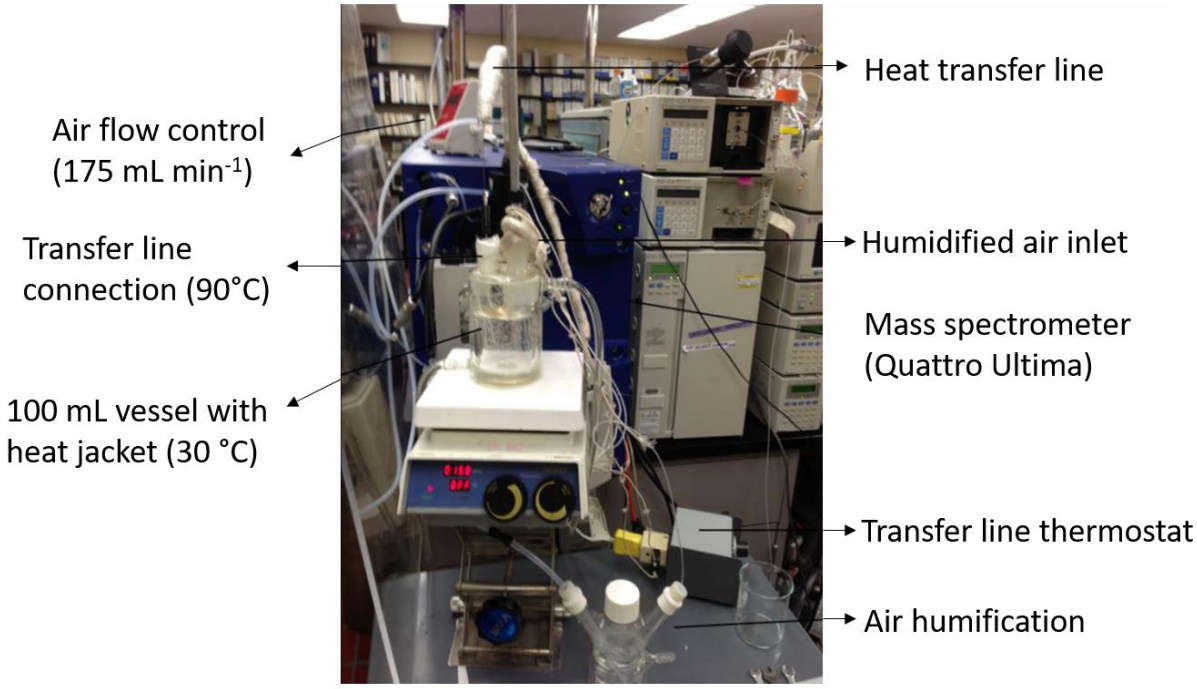

Figure A.2. Image of the APcI setup used to evaluate limonene in Chapter 4.

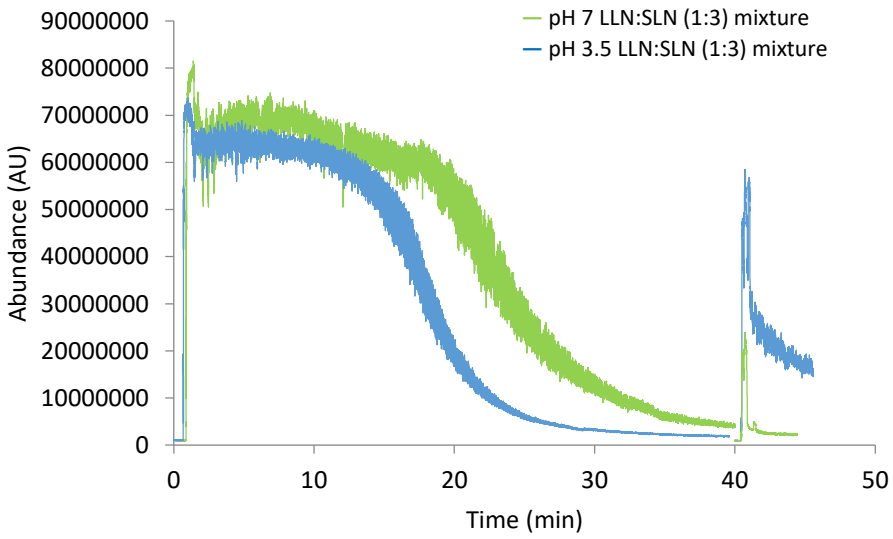

Figure A.3. Atmospheric pressure chemical ionization (APcI) plot of limonene release in colloidosomes in Chapter 4.

Reference

R. V. Potineni, D.G. Peterson, Influence of Flavor Solvent on Flavor Release and Perception in Sugar-Free Chewing Gum, J. Agric. Food Chem. 56 (2008) 3254–3259. doi:10.1021/jf072783e.

A.3. Preliminary particle size data for emulsions in Chapter five

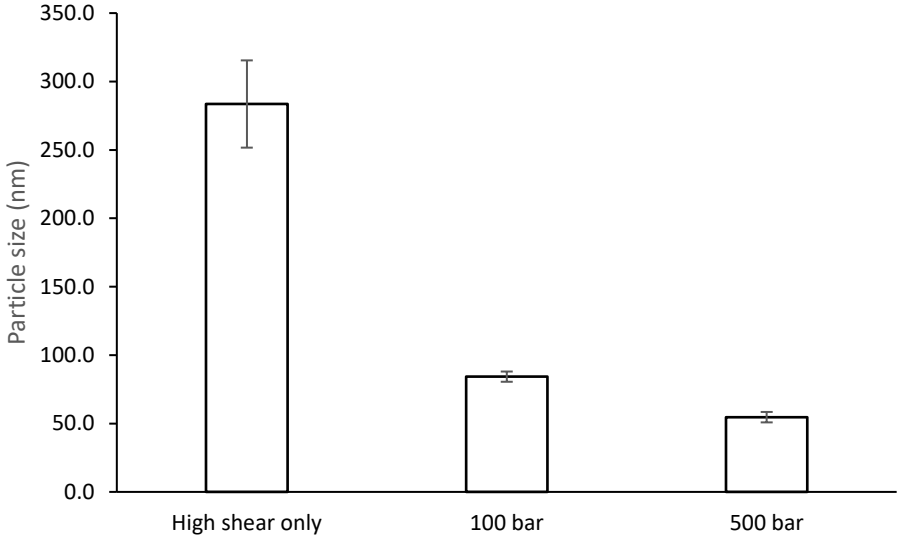

Figure A.5. Particle size of 4% PC75 lecithin homogenized with crude homogenization (high shear mixing), crude homogenization and high-pressure homogenization at 100 bar, or crude homogenization and high-pressure homogenization at 500 bar. Nanovesicles were prepared as described in Chapter 5.

A.4. Thiobarbituric acid reactive substances in ground beef

Liposomes loaded with hydrophilic (1 wt% rosemary extract) and hydrophobic (1 wt% tocopherol) antioxidants were homogenized at 500 bar (where the second stage is set to 50 bar and the total pressure is set to 500 bar with the first stage) with 4 wt% lipoid PC75 lecithin to form dispersions. The particle size of PC75 with neither rosemary extract nor tocopherol was 52.8 ± 11.5 nm; this value did not change when rosemary extract was added. When tocopherol was added prior to homogenization, the dispersions were 120.8 ± 12.5 nm.

To study the effect of the dispersions loaded with these antioxidants, 5 g of ground beef was treated with either 1 g of either PC75 homogenized with no addition, PC75 with rosemary extract, PC75 homogenized with 1 wt% tocopherol, 1% rosemary solution, or 1% tocopherol solution. The samples were mixed and sampled for thiobarbituric acid reactive substances (TBARS) 0, 1, 3, and 7 days from the addition of the PC75 dispersions. Briefly, the TBARS assay was done by adding the 1 g of the ground beef mixtures with 2.5 mL water, 2 mL TBA solution (0.05 mol L^{-1} thiobarbituric acid in 1 mol L^{-1} phosphoric acid) and 2 mL 20% trichloroacetic acid. The tubes were mixed by vortex and placed into a water bath (95°C) for 15 min. The samples were then centrifuged (3200 g for 15 min) and the supernatant was measured for absorbance at 530 nm. The spectrophotometer was blanked with the water, TBA, and trichloroacetic acid solution. TBA values were calculated by equation 2:

$$\boldsymbol{TBA} = \frac{\mathbf{50}*(\boldsymbol{Abs\ Sample - Abs\ TBARS\ solution})}{\boldsymbol{g}} \qquad (2)$$

Where 50 is a conversion factor for a 10 mm cuvette, Abs Sample is the absorbance of the supernatant, Abs TBARS solution is the absorbance of the unreacted TBARS solution, and g is the sample mass in grams. The TBAR values are presented in Figure A.6.

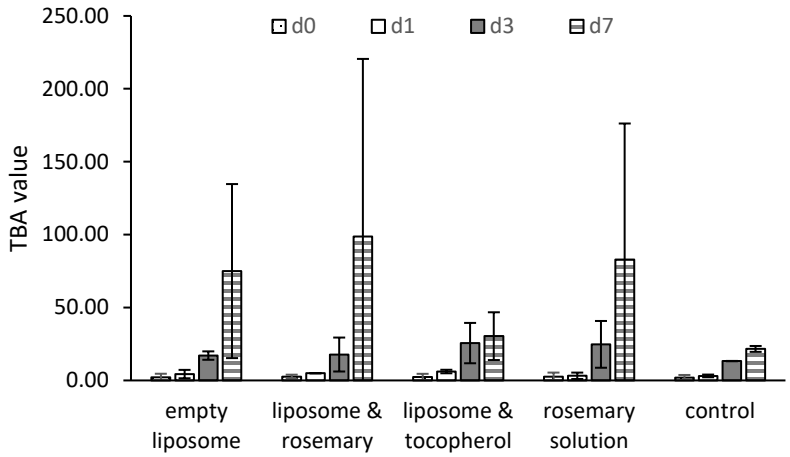

Figure A.6. TBARS values for ground beef with 4% PC75 liposomes homogenized with no addition, 4% PC75 liposomes homogenized 1% rosemary extract, 4% PC75 liposomes homogenized 1% tocopherol, 1% rosemary extract solution, 1% tocopherol solution, or control (no treatment) in ground beef over the course of 7 days. Values are the average of two replicates ± standard deviation.

A.5. 2,2-Diphenyl-1-picrylhydrazyl (DPPH) assay of hydrophobic and hydrophilic antioxidants in nanovesicles

To study the effect of hydrophilic antioxidants encapsulated into saturated and unsaturated lecithins, liposomal nanovesicles were made by homogenizing with 1% tocopherol extract solution and 4% of either Lipoid Phospholipon 80H, Lipoid Phospholipon 90G, Lipoid Phospholipon PC75, or Lipoid Phospholipon 90H at 500 bar (where the second stage is set to 50 bar and the total pressure is set to 500 bar with the first stage).

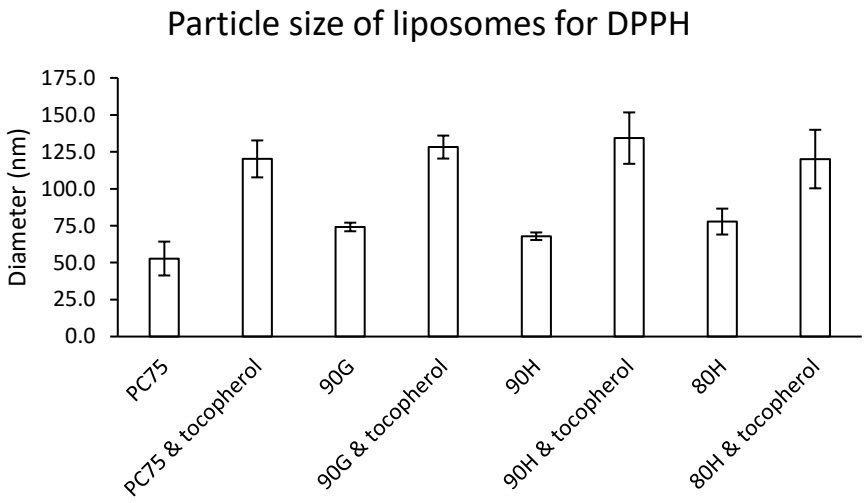

Figure A.7. Particle size of nanovesicles with and without 1% tocopherol added before homogenization.

To evaluate the performance of the dispersions, the 2,2-diphenyl-1-picrylhydrazyl (DPPH) assay was used. This method is described in in the AOAC Official Method 2012.04 antioxidant activity in foods and beverages. Briefly, the 10, 20, or 30 µL of dispersion was added to 10 mL of 40 mg L^{-1} DPPH in 50% water and 50% methanol and allowed to react for 4 h. All sample tubes were wrapped with aluminum foil. Samples were filtered with a 0.22 µm syringe filter and read for their absorbance at 517 nm. The absorbance is directly reported in Figure A.8.

For each lecithin the particle size increased with the addition of tocopherol (Figure A.7). When carrier lipid was added to nanovesicles in Chapter 5, the particle size of nanovesicles increased also for all lecithins except 90G. Comparing the antioxidant scavenging capacity of the dispersions, PC75 saw an increasing radical scavenging capacity with an increased addition of the dispersion used in the assay. Tocopherol in 90G did not greatly differ from the unloaded 90G dispersions. On the other hand, tocopherol in either saturated (90H and 80H) did not further increase the free radical scavenging capacity from the 20 to 30 µL. Although a hydrophobic spin

probe reacted at a lesser rate in 90H nanovesicles in Chapter 5, the DPPH assay displays improved free radical scavenging when tocopherol was loaded into 90H dispersions.

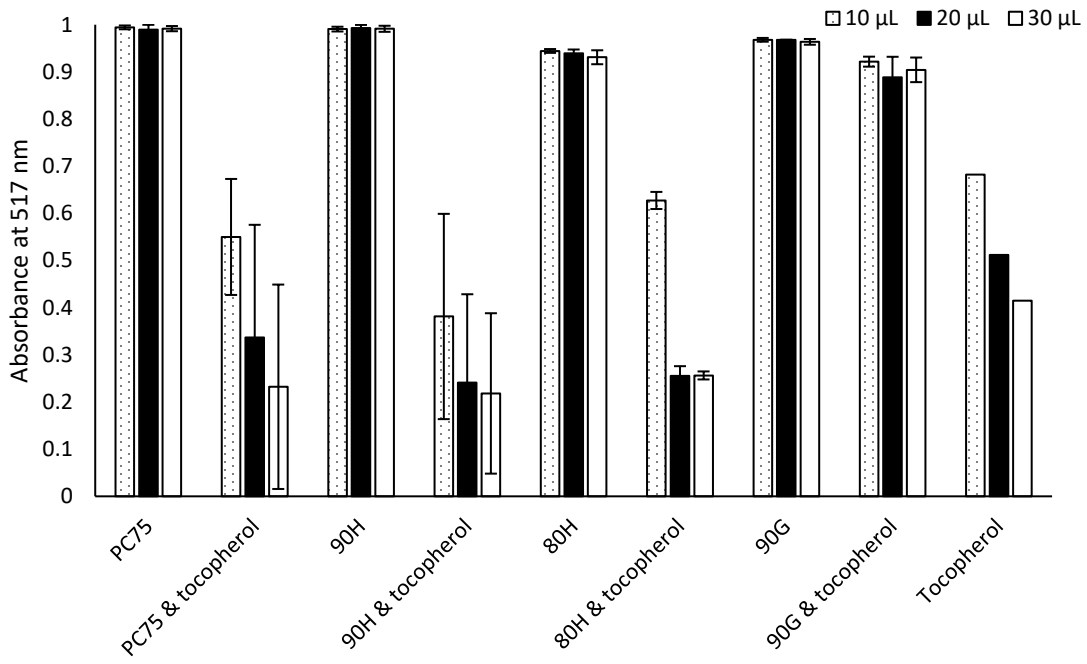

Figure A.8. 2,2'-Diphenyl-1-picrylhydrazyl (DPPH) assay of nanovesicles made with or without 1% tocopherol. Values are the average of two replicates ± standard deviation.

A.6. Formation of colloidosome structures with pectin-stabilized liquid lipid emulsions as the core particles.

Formation of colloidosomes by self-assembly of negatively charged pectin emulsions with positively charged caseinate emulsions was investigated at pH 3.5 and 7. Pectin emulsions (2 wt% pectin and 10 wt% refined coconut oil) and caseinate solid lipid nanoparticles (SLN; 4 wt% sodium caseinate and 40% palm oil) were mixed by high shear mixing with an Ultra Torrax, Ika Works, Wilmington, NC) at 24,000 rpm for 1 min and fine homogenization in a two-stage homogenizer (Panda Plus 2000, GEA Niro Soavi, Parma, Italy) at 500 bar (where the second stage

is set to 50 bar and the total pressure is set to 500 bar with the first stage), ca. 65°C, for 3 passes. The resultant emulsions were mixed at a ratio of 1:6 (pectin emulsion: caseinate SLN) at both pH 3.5 and pH 7. Emulsions and the 1:6 mixture were measured for particle size (Figure A.9) and zeta potential (Figure A.10). An indication of self-assembly between pectin emulsions and caseinate SLN is particle size of the 1:6 mixture is a greater value at pH 3.5 compared to the particle size at pH 7. Indeed, the overall zeta potential is of the 1:6 mixture has a positive zeta potential at pH 3.5 while it has a negative value at pH 7.

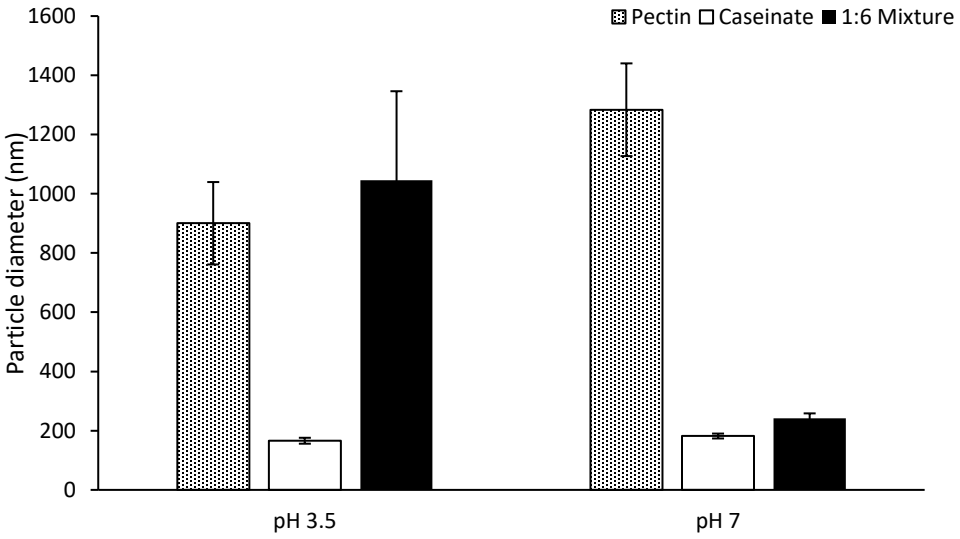

Figure A.8. Particle size of pectin emulsions, caseinate SLN, and their 1:6 mixture at pH 3.5 and 7. Values are the average of three replicates ± standard deviation.

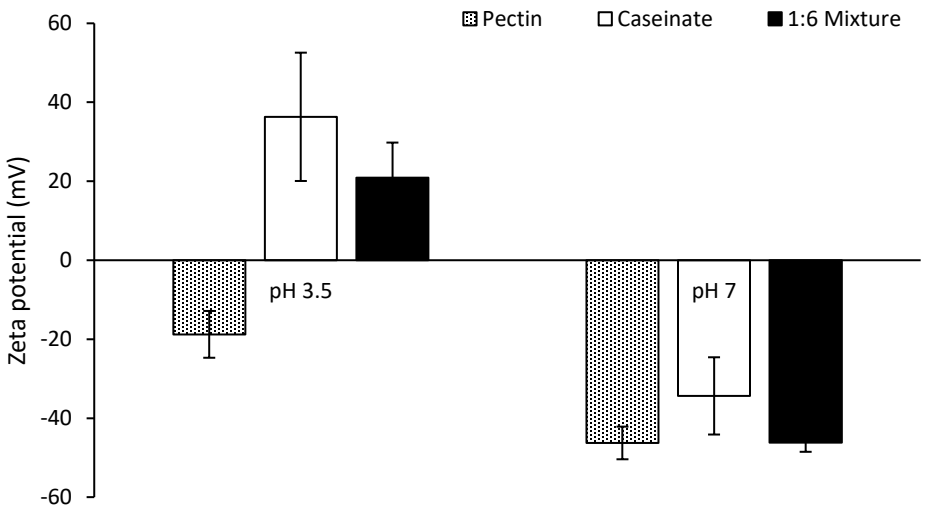

Figure A.9. Zeta potential of pectin emulsions, caseinate SLN, and their 1:6 mixture at pH 3.5 and 7. Values are the average of three replicates ± standard deviation.

To investigate the transport kinetics of a model hydrophobic ingredient from the pectin emulsion and the 1:6 mixture, 4-phenyl-2,2,5,5-tetramethyl-3-imidazoline-1-oxyl nitroxide (PTMIO) was added to the pectin emulsions prior to homogenization. The samples were analyzed under the following measurement conditions: center field 335.5 mT, sweep width 6.0 mT, modulation frequency 100 kHz, modulation amplitude 100 uT, microwave power 6.3 mW. The reduction kinetics of PTMIO were monitored by the ascorbate reaction described in Chapter 4. Briefly, sodium ascorbate (2 mM) and ferric chloride (10 μM) were added to samples (10 mL) under deoxygenated conditions to reduce PTMIO to its EPR-silent form. Within 30 seconds of the addition of the reagents, aliquots of the mixture (50 μL) were collected in sealed borosilicate capillary tubes. EPR spectra were collected at 2-minute intervals over 30 minutes (Figure A.10). Pectin emulsions had first order reaction rate constants of $2.65 \pm 0.244 \times 10^{-3}\ min^{-1}$ and $1.95 \pm 0.593 \times 10^{-3}\ min^{-1}$ at pH 3.5 and 7, respectfully. The 1:6 mixture had $1.66 \pm 0.688 \times 10^{-3}\ min^{-1}$ and $2.35 \pm 0.308 \times 10^{-3}\ min^{-1}$ at pH 3.5 and 7, respectfully.

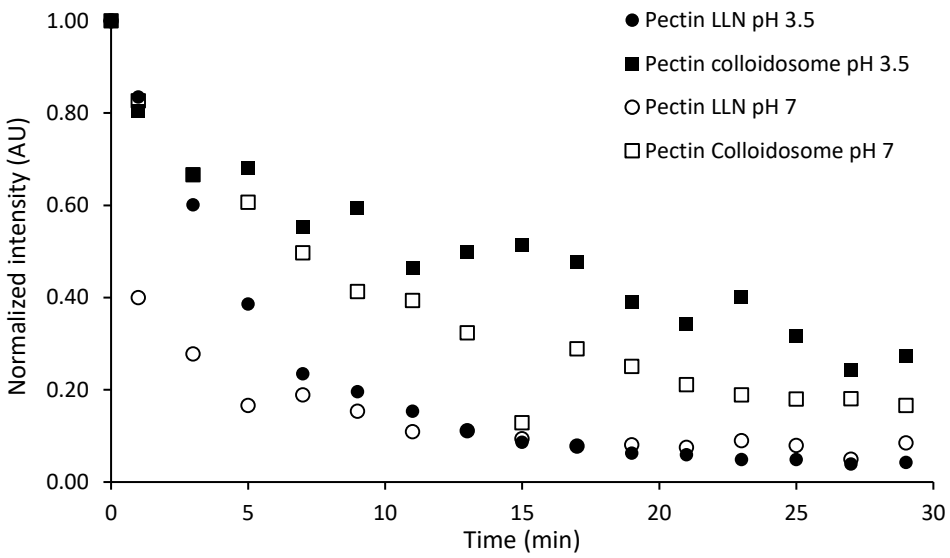

Figure A.10. Reduction of PTMIO in pectin emulsions and the 1:6 (pectin emulsion: caseinate SLN) mixture at pH 3.5 and 7. Values are the average of three replicates ± standard deviation.